Article

Cell Systems

Critical Roles of the Pentose Phosphate Pathway and *GLN3* in Isobutanol-Specific Tolerance in Yeast

Graphical Abstract

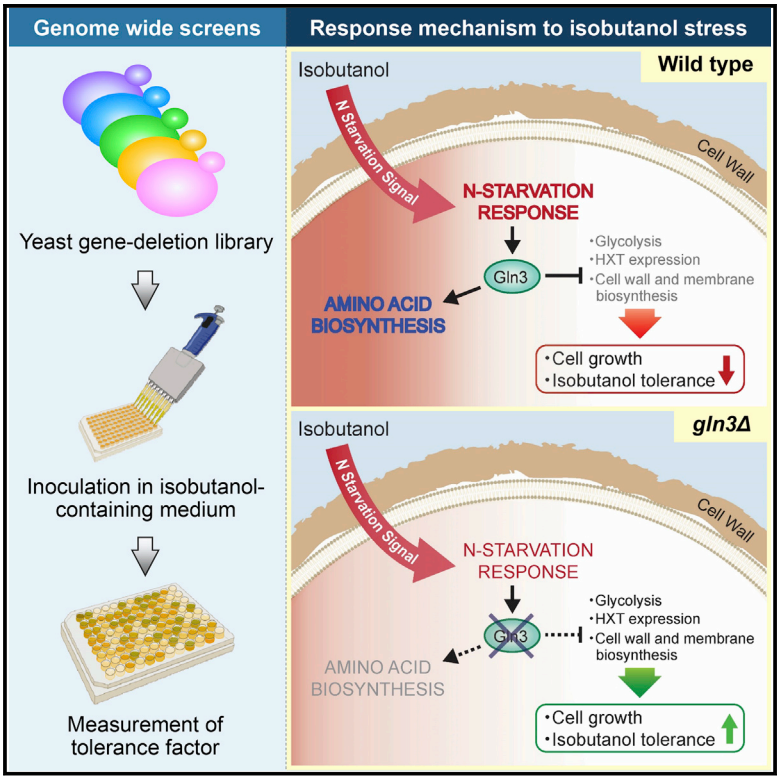

Highlights

- Deletion of pentose phosphate pathway genes causes isobutanol hypersensitivity
- Deletion of *GLN3* increases yeast tolerance specifically to branched-chain alcohols
- Isobutanol production is greatly increased by deleting *GLN3* in engineered strains
- The nitrogen starvation response induced by isobutanol is evaded in *gln3Δ* strains

Authors

Kouichi Kuroda, Sarah K. Hammer, Yukio Watanabe, ..., Gregory Stephanopoulos, Mitsuyoshi Ueda, José L. Avalos

Correspondence

k_kuro@kais.kyoto-u.ac.jp (K.K.), javalos@princeton.edu (J.L.A.)

In Brief

This study provides insights into the yeast response to isobutanol and mechanisms underlying specific toxicity and tolerance to isobutanol. Deletion of *GLN3* markedly increases yeast tolerance specifically to branched-chain alcohols and isobutanol production. Deletion of *GLN3* evades the native nitrogen starvation response induced by isobutanol, enhancing isobutanol tolerance. These findings illustrate how adaptive mechanisms to tolerate stress can lead to toxicity in chemical production and provide a promising strategy to boost production by genetically disrupting such mechanisms.

Kuroda et al., 2019, Cell Systems *9*, 1–14
December 18, 2019
https://doi.org/10.1016/j.cels.2019.10.006

CellPress

Please cite this article in press as: Kuroda et al., Critical Roles of the Pentose Phosphate Pathway and *GLN3* in Isobutanol-Specific Tolerance in Yeast, Cell Systems (2019), https://doi.org/10.1016/j.cels.2019.10.006

Cell Systems
Article

Critical Roles of the Pentose Phosphate Pathway and *GLN3* in Isobutanol-Specific Tolerance in Yeast

Kouichi Kuroda,[1,7,*] Sarah K. Hammer,[2,7] Yukio Watanabe,[1] José Montaño López,[2] Gerald R. Fink,[3] Gregory Stephanopoulos,[4] Mitsuyoshi Ueda,[1] and José L. Avalos[2,5,6,8,*]
[1]Division of Applied Life Sciences, Graduate School of Agriculture, Kyoto University, Kitashirakawa Oiwake-cho, Sakyo-ku, Kyoto, Japan
[2]Department of Chemical and Biological Engineering, Princeton University, Princeton, NJ, USA
[3]Whitehead Institute for Biomedical Research, Cambridge, MA, USA
[4]Department of Chemical Engineering, Massachusetts Institute of Technology, Cambridge, MA, USA
[5]Andlinger Center for Energy and the Environment, Princeton University, Princeton, NJ, USA
[6]Department of Molecular Biology, Princeton University, Princeton, NJ, USA
[7]These authors contributed equally
[8]Lead Contact
*Correspondence: k_kuro@kais.kyoto-u.ac.jp (K.K.), javalos@princeton.edu (J.L.A.)
https://doi.org/10.1016/j.cels.2019.10.006

SUMMARY

Branched-chain alcohols are attractive advanced biofuels; however, their cellular toxicity is an obstacle to engineering microbes to produce them at high titers. We performed genome-wide screens on the *Saccharomyces cerevisiae* gene deletion library to identify cell systems involved in isobutanol-specific tolerance. Deletion of pentose phosphate pathway genes *GND1* or *ZWF1* causes hypersensitivity to isobutanol but not to ethanol. By contrast, deletion of *GLN3* increases yeast tolerance specifically to branched-chain alcohols. Transcriptomic analyses revealed that isobutanol induces a nitrogen starvation response via *GLN3* and *GCN4*, upregulating amino acid biosynthesis and nitrogen scavenging while downregulating glycolysis, cell wall biogenesis, and membrane lipid biosynthesis. Disruption of this response by deleting *GLN3* is enough to enhance tolerance and boost isobutanol production 4.9-fold in engineered strains. This study illustrates how adaptive mechanisms to tolerate stress can lead to toxicity in microbial fermentations for chemical production and how genetic interventions can boost production by evading such mechanisms.

INTRODUCTION

Concerns about climate change have motivated efforts to engineer microbes to convert renewable feedstocks into fuels and chemicals typically derived from petroleum. In order to develop economically competitive production processes for commodity fuels and chemicals, it is critical to obtain the highest yields, titers, and productivities possible. A major barrier to the cost-effective production of microbial fuels and chemicals is the cellular toxicity of the products of interest, which limits the maximum titers that can be achieved. It has been shown that improving microbial tolerance to toxic products can lead to higher production (Mukhopadhyay, 2015; Qiu and Jiang, 2017). However, the development of strains with improved tolerance, and potentially increased production, is hampered by the complex and diverse nature of microbial responses to toxic products, leaving many microbial tolerance mechanisms uncharacterized.

Isobutanol and other branched-chain alcohols, such as isopentanol and 2-methyl-1-butanol, are promising advanced biofuels that could be used as gasoline substitutes, or upgraded to jet fuel (Brooks et al., 2016; Dürre, 2007; Park et al., 2015). These molecules have superior fuel properties to ethanol, including higher energy density, lower hygroscopicity, and lower volatility that result in increased compatibility with current fuel infrastructure. The yeast *Saccharomyces cerevisiae* is an attractive host for branched-chain alcohol production because of its facile genetic manipulation, ability to grow at low pH, immunity to phage contamination, and ease of separation (Kuroda and Ueda, 2016). Another key advantage is that *S. cerevisiae* is currently employed in the majority of large-scale bioethanol production processes, which provides an opportunity to simplify and expedite the transition to large-scale production of advanced biofuels by retrofitting existing bioethanol facilities. Furthermore, *S. cerevisiae* has an inherent ability to produce small amounts of branched-chain alcohols as products of amino acid degradation and may have evolved mechanisms to better tolerate these products. These advantages have motivated efforts to engineer yeast for branched-chain alcohol production (Avalos et al., 2013; Brat et al., 2012; Hammer and Avalos, 2017; Matsuda et al., 2013; Park et al., 2016; Tan et al., 2016; Zhao et al., 2018).

Although *S. cerevisiae* is naturally highly tolerant to ethanol, enduring concentrations as high as 18% (v/v) (Liu and Qureshi, 2009), it is still sensitive to ethanol's toxic effects. Previous studies have shown that ethanol primarily affects cell membranes (Stanley et al., 2010). By increasing membrane fluidity, ethanol decreases membrane integrity (Lloyd et al., 1993; Mishra and Prasad, 1989) and increases ion permeability, perturbing proton homeostasis (Madeira et al., 2010). Adding potassium

or buffers to limit acidification of the media increases yeast tolerance to ethanol, boosting ethanol titers. This effect can be reproduced genetically by increasing the activity of *TRK1* (a K^+ importer) and overexpressing *PMA1* (a H^+ exporter), indicating that ion homeostasis plays an important role in ethanol sensitivity (Lam et al., 2014). Beyond toxicity to the cell membrane, loss of normal vacuolar function or structure can cause increased ethanol sensitivity, implicating protein turnover and ion homeostasis in the ethanol stress response (Kubota et al., 2004; Stanley et al., 2010; Yoshikawa et al., 2009). Lastly, overexpression of genes involved in tryptophan biosynthesis (Hirasawa et al., 2007), and genes with binding sites for transcription factors Msn4p/Msn2p, Yap1p, Hsf1p, and Pdr1p/Pdr3p (Ma and Liu, 2010), increase ethanol tolerance.

Considerably less is understood about the mechanisms of toxicity and cell response induced by higher alcohols in yeast. Yet, it is known that butanol isomers are much more toxic than ethanol to yeast cells (Knoshaug and Zhang, 2009). Similar to ethanol, 1-butanol affects membrane lipid composition (Huffer et al., 2011) and nutrient transport, (Leão and van Uden, 1982) in addition to inhibiting initiation of translation (Ashe et al., 2001). However, a tolerance mechanism specific for higher alcohols has been described, in which genes involved in protein degradation are important for cell tolerance to butanol isomers but not to ethanol (González-Ramos et al., 2013). Isobutanol toxicity in yeast is even less understood, with one study revealing that knockdown of the Hsp70 family of heat shock proteins increases isobutanol tolerance (Crook et al., 2016) and patents claiming that isobutanol tolerance is enhanced by deleting *GCN* genes (LaRossa, 2013) or overexpressing the transcription factor *MSS11* (Bramucci et al., 2013). Proteins involved in mitochondrial respiration and glycerol biosynthesis, identified for their ability to increase tolerance to 2-butanol, also appear beneficial for isobutanol tolerance (Ghiaci et al., 2013). While data suggest that there are some commonalities in the toxicity responses to different alcohols in *S. cerevisiae* (Fujita et al., 2006) and *Escherichia coli* (Chen et al., 2018), response mechanisms in both microbes depend on the chain length and structure of alcohols (Dunlop, 2011; Fujita et al., 2006). Thus, ethanol tolerance cannot be used as an accurate predictor of yeast tolerance to isobutanol or other higher alcohols.

Here, we use the yeast gene deletion library (Giaever et al., 2002; Winzeler et al., 1999) to study the specific tolerance of *S. cerevisiae* to isobutanol. We identified several genes in the pentose phosphate pathway (PPP) that are implicated in yeast specific tolerance to higher alcohols (C4–C6). We also found that deletion of *GLN3* significantly boosts yeast tolerance specifically to higher branched-chain alcohols, but not to simple alcohols (including ethanol) or higher linear alcohols. Transcriptomic analyses revealed that increased isobutanol tolerance in the *GLN3* deletion strain is linked to downregulation of *GCN4*-regulated genes involved in biosynthesis of amino acids. Furthermore, we show that engineering the isobutanol biosynthetic pathway in hypertolerant strains containing the *GLN3* deletion boosts isobutanol titers by as much as 4.9-fold. This study reveals the pathways in yeast involved in specific tolerance to isobutanol and other higher alcohols and demonstrates how isobutanol production can be substantially increased in isobutanol-tolerant strains.

RESULTS

Estimating LC_{50} for Isobutanol in Liquid and Solid Media

Our first step was to identify the LC_{50} (lethal concentration for 50% of cells) of isobutanol for the BY4741 wild-type strain, from which the gene deletion library was developed (Giaever et al., 2002; Winzeler et al., 1999). Screening the gene deletion library using isobutanol concentrations near the LC_{50} ensures that the concentration is high enough to probe changes in isobutanol tolerance across different strains in the collection but below the concentration that would be lethal to all deletion strains. We monitored cell growth of BY4741 in synthetic complete (SC) liquid medium containing concentrations of isobutanol ranging from 0.0% to 1.8% (v/v), by measuring the optical density at 600 nm (OD_{600}) after 24-h cultivation. Cell growth was marginally affected at concentrations below 1.3% but was considerably inhibited at those above 1.6% (Figure S1A). Isobutanol concentrations of 1.4% and 1.5% caused moderate inhibition, with 1.5% isobutanol reducing wild-type growth by slightly more than half, thereby approximating the LC_{50} (Figure S1A). To evaluate isobutanol growth inhibition on solid medium, we spotted serial dilutions of BY4741 onto agar plates containing varying concentrations of isobutanol. On agar plates containing 2.4% isobutanol, cell growth is still observable but noticeably inhibited (Figure S1B). The higher LC_{50} determined from agar plates may be the result of higher cell tolerance to isobutanol in solid media; alternatively, it could reflect the difficulty in accurately preparing solid media with isobutanol due to isobutanol evaporation during the pouring of hot agar.

Screen for Deletion Strains with Increased Sensitivity or Tolerance to Isobutanol

Based on these results, we screened the BY4741 gene deletion library (Giaever et al., 2002; Winzeler et al., 1999) for changes in cell growth in liquid SC medium containing 1.4% (v/v) isobutanol. At this conservative concentration (slightly lower than the apparent LC_{50}), we were able to identify gene deletion strains with increased sensitivity or tolerance to isobutanol relative to wild type. To quantify these phenotypes, we defined a tolerance factor as the ratio of the OD_{600} of cells grown with isobutanol in the medium after 24 h, divided by the OD_{600} of cells grown in the absence of isobutanol for the same amount of time. Thus, we classified deletion strains as having increased sensitivity or tolerance to isobutanol based on the comparison of their tolerance factors to that of the wild-type strain in 1.4% isobutanol measured during the screen (Table S1). This initial screen identified 1,025 strains with increased sensitivity (tolerance factor < 0.2) and 517 strains with enhanced tolerance (tolerance factor > 0.8), (Figure 1A and Table S2).

The 1,542 strains with a tolerance factor lower than 0.2 or greater than 0.8 identified in the initial screen were subjected to a second screen to find those with hypersensitivity or hypertolerance to isobutanol. The 1,025 sensitive strains were grown in lower isobutanol concentrations (1.2% and 0.6%) to identify those exhibiting substantial growth inhibition even at reduced isobutanol concentrations. This screen was repeated for the 164 most sensitive strains identified in the second screen (Figure 1B; Table S3). In a similar manner, the 517

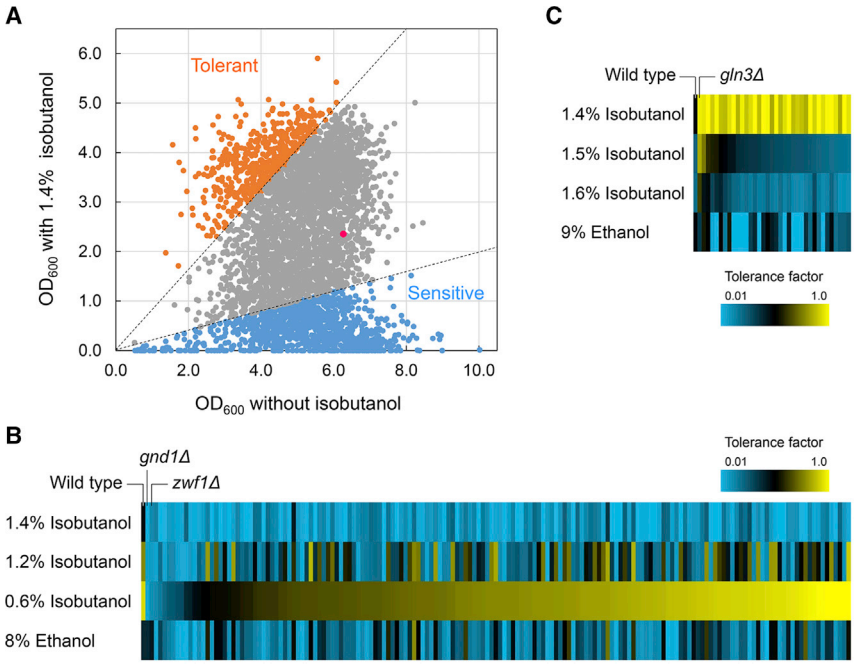

Figure 1. Screens for Deletion Strains with Increased Sensitivity or Tolerance to Isobutanol

(A) Optical density (OD_{600}) measurements of deletion library strains grown in liquid cultures in the presence or absence of 1.4% (v/v) isobutanol. Strains with enhanced tolerance, with a tolerance factor > 0.8, are indicated in orange; strains with increased sensitivity, with a tolerance factor < 0.2, are indicated in blue; the wild-type strain is indicated in red.

(B) Heatmap of tolerance factors of the 164 sensitive strains identified in the second screen (Table S3) and the wild-type strain, grown in 1.4% isobutanol, 1.2% isobutanol, 0.6% isobutanol, or 8% ethanol. After the wild-type data in the leftmost position, data are shown in ascending order based on tolerance factors in the 0.6% isobutanol condition.

(C) Heatmap of tolerance factors of the 36 tolerant strains identified in the second screen (Table S4) and the wild-type strain, grown in 1.4% isobutanol, 1.5% isobutanol, 1.6% isobutanol, or 9% ethanol. After the wild-type data in the leftmost position, data are shown in descending order based on tolerance factors in the 1.5% isobutanol condition. See also Figure S1; Tables S1, S2, S3–S5.

tolerant strains were grown in higher concentrations of isobutanol (1.5% and 1.6%) to identify the most tolerant strains. This screen was repeated for the 36 most tolerant strains identified in the second screen (Figure 1C; Table S4). To assess the specificity of changes in tolerance to isobutanol, we also measured the growth of these selected strains in media containing ethanol: 8% for sensitive strains or 9% for tolerant strains. Out of the 164 sensitive strains, we categorize the 46 strains that continue to display increased sensitivity to isobutanol at lower concentrations (tolerance factor < 0.5 in 0.6% isobutanol or tolerance factor < 0.1 in 1.2% isobutanol) as hypersensitive (Table S3). Among the 36 strains with increased tolerance, 6 continue to display increased tolerance (tolerance factor > 0.4) in 1.5% isobutanol, which we categorize as hypertolerant (Table S4).

Next, we performed a Gene Ontology (GO) enrichment analysis of genes deleted in the 164 most sensitive and 36 most tolerant strains. Although genes deleted in strains with enhanced tolerance are not enriched in any specific GO term, we found that gene deletions in strains with increased sensitivity are enriched in several biological processes, including aromatic amino acid-related processes, cellular ion homeostasis, and vacuolar functions (Table S5). In fact, five strains harboring deletions of *TRP* genes, encoding enzymes in tryptophan biosynthesis, show increased isobutanol sensitivity (with *trp2Δ*, *trp3Δ*, and *trp5Δ* being hypersensitive strains). We examined the increased sensitivity to isobutanol caused by *TRP1* deletion because it is an auxotrophic marker in commonly used strains, such as CEN.PK- and SEY6210-derived strains. These strains exhibit increased isobutanol sensitivity similar to that of the BY4741 *trp1Δ* strain in 1.3% isobutanol (Figure S1C). Furthermore, after repairing the *TRP1* allele in CEN.PK2-1C and SEY6210, wild-type (BY4741) levels of isobutanol tolerance are recovered (Figure S1C). These results suggest that tryptophan biosynthesis is important for isobutanol stress response.

Hypersensitive Strains Demonstrate Specific Sensitivity to Isobutanol and Other C4–C6 Alcohols

We measured growth of 19 hypersensitive strains in liquid SC medium containing 0.6%, 1.0%, or 1.4% isobutanol or 8% ethanol. These growth experiments were initiated at an OD_{600} of 0.1, unlike in previous screens, which started with much smaller inoculums (from a 96-pin replicator). In 1.4% isobutanol, growth of all 19 strains is strongly inhibited compared to the wild-type BY4741 strain (Figure 2A). However, in media containing 0.6% or 1.0% isobutanol, the sensitivity varies between strains. Four strains—*gnd1Δ*, *zwf1Δ*, *vps34Δ*, and *pep12Δ*—display tolerance factors less than 0.3 even in 0.6% isobutanol (Figure 2A), with *gnd1Δ* and *zwf1Δ* strains showing the greatest sensitivity. Among the hypersensitive strains, *gnd1Δ*, *zwf1Δ*, and *nha1Δ* have a unique phenotype: despite their hypersensitivity to isobutanol, they are no more sensitive to ethanol than the wild-type strain. In contrast, the other hypersensitive strains also have increased sensitivity to 8% ethanol (Figure 2A). Thus, deletion of *GND1*, *ZWF1*, or *NHA1* causes isobutanol-specific hypersensitivity in both liquid and solid media (Figures 2A and S2A). We confirmed that the isobutanol-specific hypersensitivity observed in the two most sensitive strains—*gnd1Δ* and *zwf1Δ*—is due to loss of *GND1* and *ZWF1* function, respectively, by reconstructing *GND1* and *ZWF1* gene deletions in the wild-type BY4741 strain (Figure S3A).

We then explored the sensitivity of *gnd1Δ* and *zwf1Δ* strains to other alcohols including methanol, 1-propanol, 1-butanol, 2-butanol, tert-butanol, 1-pentanol, 2-methyl-1-butanol, isopentanol, and 1-hexanol. Neither strain demonstrates notably increased sensitivity to methanol, ethanol, or 1-propanol compared to the wild-type strain. However, cell growth is substantially inhibited in the presence of all alcohols tested with four or more carbons (Figure 2B). These results indicate that *GND1* and *ZWF1* play crucial roles in cellular tolerance to C4–C6 alcohols, regardless of their branching. However,

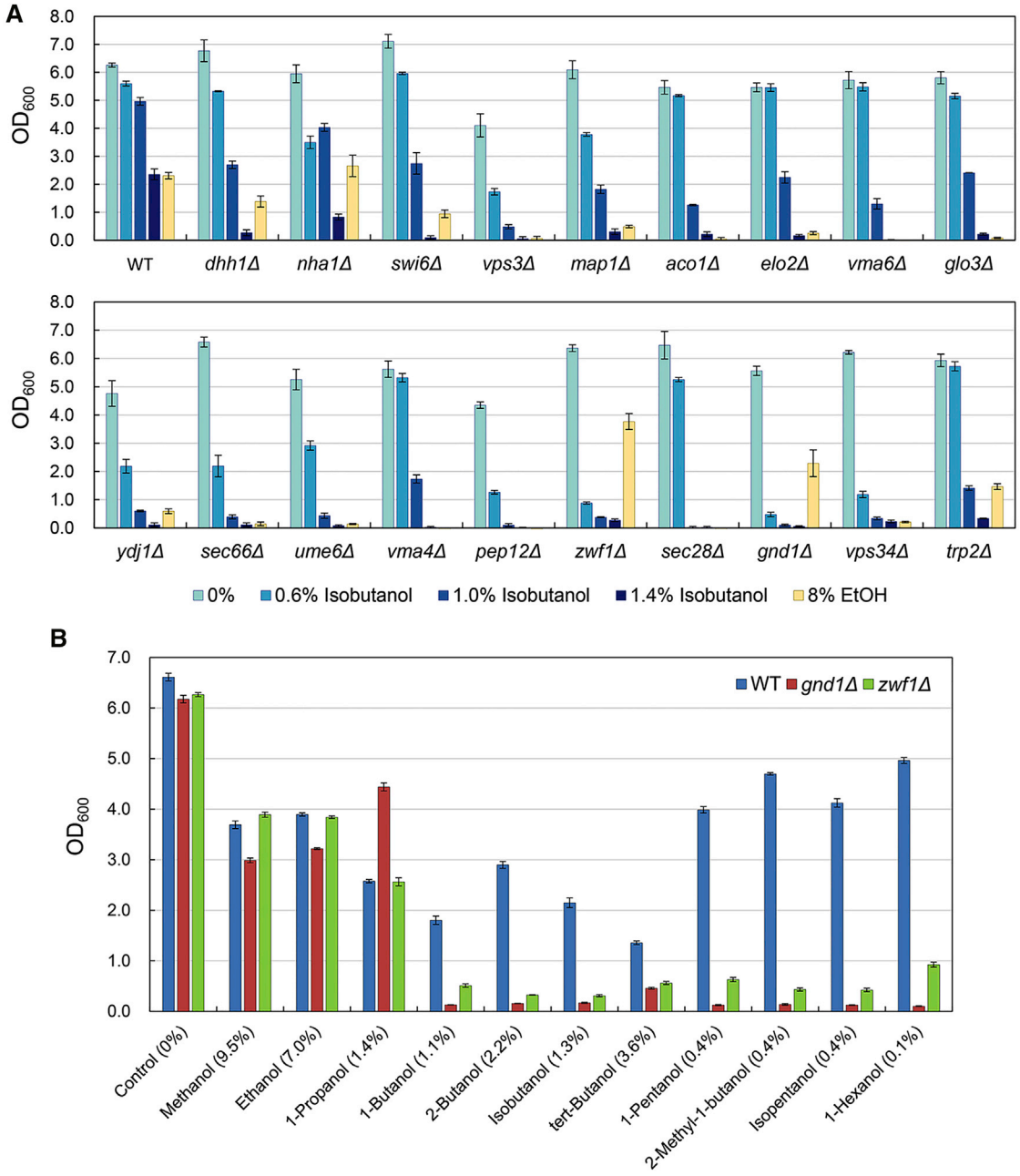

Figure 2. Strains with Hypersensitivity to Isobutanol and Other Alcohols

(A) Isobutanol and ethanol sensitivity of 19 of the deletion strains identified as hypersensitive to isobutanol in liquid medium. Error bars represent the SEM of three independent experiments.

(B) Sensitivity of BY4741 (wild type, WT), *gnd1Δ*, and *zwf1Δ* strains to various alcohols in liquid medium. The concentrations of each alcohol are indicated in parentheses (v/v). Error bars represent the SEM of three independent experiments. See also Figures S2A, S3A, and S4.

neither deletion of *GND1* nor *ZWF1* appears to affect ethanol tolerance.

The PPP Is Involved in Tolerance to Isobutanol

ZWF1 and *GND1* encode enzymes that catalyze NADPH-generating reactions, constituting the first and third steps of the PPP, respectively (Figure 3A). Measurements of intracellular NADPH/$NADP^+$ ratios revealed that the *zwf1Δ* strain has lower NADPH/$NADP^+$ ratios than the wild-type strain in medium with or without isobutanol (Figure S4). However, NADPH/$NADP^+$ ratios are relatively unchanged in the *gnd1Δ* strain compared to wild type. We also tested the isobutanol-specific sensitivity of strains lacking genes encoding other PPP enzymes that do not catalyze NADPH-generating reactions directly. We found that *rpe1Δ*

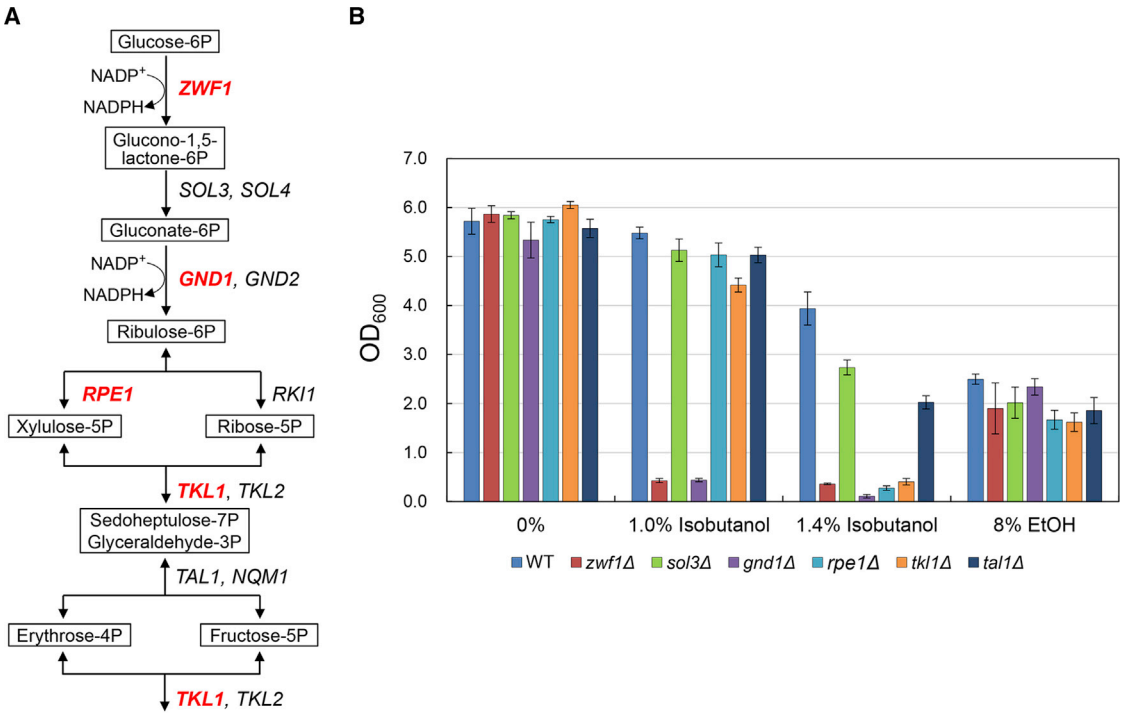

Figure 3. Involvement of the Pentose Phosphate Pathway in Yeast Tolerance to Isobutanol

(A) Schematic representation of the PPP with genes encoding constituent enzymes. Genes in red are among the 164 genes which, when deleted, cause the most sensitivity to isobutanol.

(B) Isobutanol and ethanol tolerance of strains lacking a single PPP gene. Error bars represent the SEM of three independent experiments. See also Figures S2A and S5.

and *tkl1Δ* strains have isobutanol-specific sensitivities comparable to those of the *gnd1Δ* and *zwf1Δ* strains in 1.4% isobutanol (Figure 3B). However, deletion of *GND1* or *ZWF1* causes much higher sensitivity to 1.0% isobutanol than deletion of other genes in the PPP. Although the *sol3Δ* and *tal1Δ* strains are not as sensitive to isobutanol as the *gnd1Δ* and *zwf1Δ* strains in 1.0% isobutanol, their sensitivity to 1.4% isobutanol is still greater than that of the wild-type strain (Figure 3B). None of the tested PPP deletion strains show increased sensitivity to 8% ethanol, consistent with the PPP being specifically important for higher alcohol tolerance (Figure 3B).

To test whether overexpressing genes of the PPP increases isobutanol tolerance, we transformed BY4741 with 2 μ plasmids containing single PPP genes under the control of their native promoters and terminators. Overexpression of *RPE1* or *SOL3* significantly enhances isobutanol tolerance relative to the wild-type strain with an empty plasmid; overexpression of other PPP genes causes more moderate improvements in isobutanol tolerance (Figure S5).

Deletion of *GLN3* Enhances Yeast Tolerance Specifically to Branched-Chain Alcohols

We examined the 6 hypertolerant strains in liquid medium containing 1.5% or 1.6% isobutanol or 8% ethanol. These strains—*gln3Δ*, *gnp1Δ*, *vps55Δ*, *gcn3Δ*, *avt3Δ*, and *ydr391cΔ*—grow better than the wild type in 1.5% isobutanol; *gln3Δ*, *gnp1Δ*, *vps55Δ*, and *gcn3Δ* also demonstrate enhanced tolerance in 1.6% isobutanol (Figure 4A). Notably, all six hypertolerant deletion strains are at least as sensitive to 8% ethanol as the wild-type strain. The *gln3Δ* strain can grow on SC agar medium containing 2.7% isobutanol (Figure S2B). As in liquid medium, the enhanced tolerance of these strains to isobutanol does not translate into enhanced tolerance to ethanol in solid medium (Figure S2B).

Our results show that deletion of *GLN3* confers the highest tolerance to isobutanol in liquid and solid medium, with OD_{600} values more than three times those of the wild-type strain in liquid medium (Figure 4A). *GLN3* encodes a transcriptional activator that, in response to nitrogen deprivation, induces the expression of genes that are subjected to nitrogen catabolite repression in the presence of high-quality nitrogen sources (Courchesne and Magasanik, 1988; Magasanik and Kaiser, 2002). We confirmed that the isobutanol-specific hypertolerance of the *gln3Δ* strain was due to loss of the *GLN3* gene by reconstructing *GLN3* deletions in the parent CEN.PK2-1C (with *TRP1* restored) and BY4741 strains (Figures S3B and S3C).

Next, we explored tolerance of the *gln3Δ* strain to other alcohols by measuring its growth in liquid medium containing methanol, 1-propanol, 1-butanol, 2-butanol, tert-butanol, 1-pentanol, 2-methyl-1-butanol, isopentanol, or 1-hexanol (Figure 4B). Compared to the wild-type strain, the *gln3Δ* strain has dramatically enhanced tolerance to branched-chain alcohols (isobutanol, tert-butanol, 2-methyl-1-butanol, and isopentanol), with an OD_{600} as much as 11.4-fold higher in the presence of 0.55% 2-methyl-1-butanol. A smaller, but statistically significant, increase in tolerance is observed in the presence of the linear

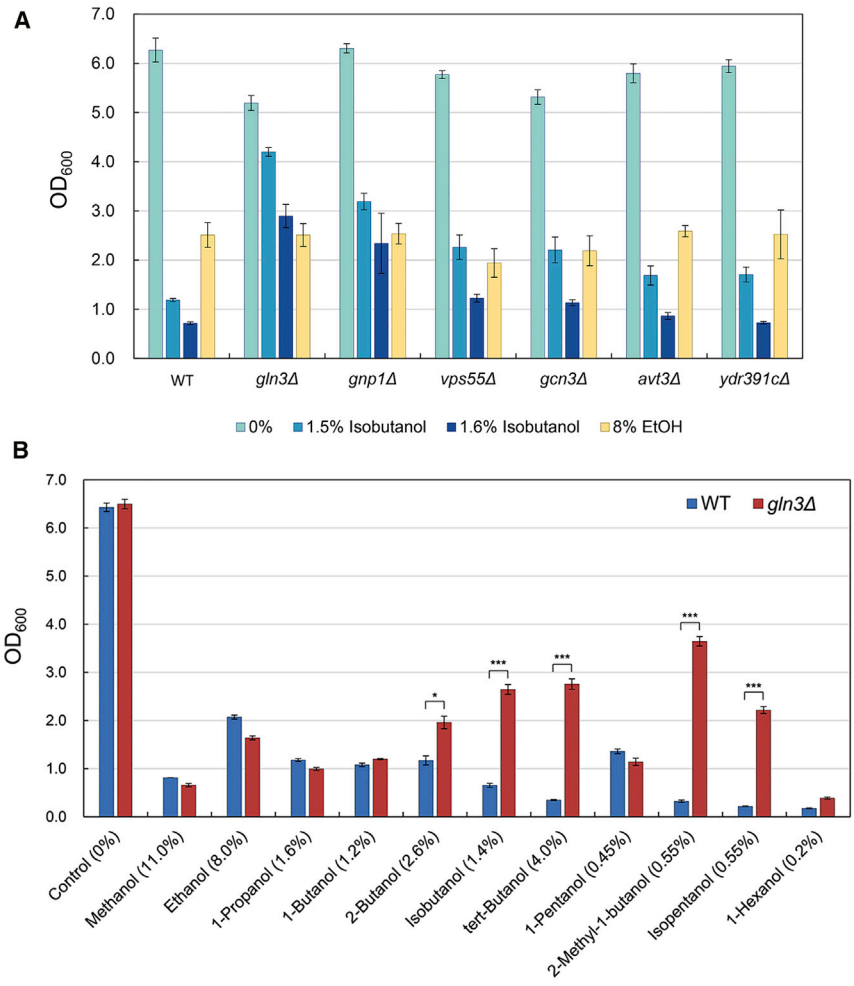

Figure 4. Enhanced Tolerance of the *gln3Δ* Strain to Branched-Chain Alcohols

(A) Isobutanol and ethanol tolerance of the six hypertolerant strains in liquid medium. Error bars represent the SEM of three independent experiments.

(B) Tolerance of the *gln3Δ* strain to various alcohols in liquid medium. The concentrations of each alcohol are indicated in parentheses (v/v). Error bars represent the SEM of three independent experiments. A two-tailed Student's t test was used to assess the statistical significance of the difference between cell growths of wild-type and *gln3Δ* strains in the presence of branched-chain alcohols; *p < 0.01, **p < 0.001, ***p < 0.0001. See also Figures S2B, S3B, S3C, S4, S8, and S9.

secondary alcohol, 2-butanol. However, the *gln3Δ* strain does not increase tolerance to the linear primary alcohols 1-propanol, 1-butanol, 1-pentanol, and 1-hexanol or the short-chain alcohols methanol and ethanol; in fact, the *gln3Δ* strain is more sensitive to some of these alcohols than the wild-type strain (Figure 4B). Therefore, deletion of *GLN3* confers enhanced tolerance specifically to branched-chain higher alcohols.

Transcriptomic Analyses of the Wild-Type and *gln3Δ* Strains Reveal a Mechanism for Isobutanol Sensitivity and Tolerance

To elucidate underlying mechanisms responsible for enhanced isobutanol tolerance of the *gln3Δ* strain, we used RNA-seq to compare the transcriptomic profiles of wild-type and *gln3Δ* strains grown with or without 1.3% isobutanol (Table S6). We used the natural response of the wild-type strain to isobutanol as our baseline for analysis (Figure 5A; Tables S7A and S7B). We observe that the largest group of genes induced by isobutanol in the wild-type strain belongs to cellular amino acid metabolic processes, followed by genes involved in transmembrane transport, including seven genes encoding putative or confirmed transporters of amino acids (Figures 5A and S6A; Table S7A). Conversely, isobutanol represses several genes associated with glucose uptake and cell growth, such as genes encoding hexose transporters (*HXT2*, *HXT4*, *HXT5*, and *HXT6*) and proton pumps (*PMA1* and *PMA2*) as well as genes involved in glycolysis, the pentose phosphate pathway, and cell wall biogenesis (Figures 5A and S6B; Table S7B). Therefore, it seems that isobutanol triggers a nitrogen deprivation response in the wild-type strain even in the presence of rich nitrogen sources.

In contrast, the *gln3Δ* strain is unable to induce a nitrogen starvation response in the presence of isobutanol (Figures S6A and S7A; Table S7C). Instead, it induces most notably genes involved in cell wall biogenesis and ion transport (Table S7C). Moreover, the *gln3Δ* strain does not repress genes involved in glycolysis in the presence of isobutanol as the wild type does (Figures S6B and S7A; Table S7D). Comparing the transcriptomes of the *gln3Δ* and wild-type strains grown without isobutanol, genes involved in chemical responses account for the largest number of genes expressed more highly in the *gln3Δ* strain (Table S7E). However, an even larger number of genes belonging to this GO term show lower levels of expression in the *gln3Δ* relative to wild type (Table S7F); thus, it is difficult to identify which transcriptomic changes between these strains in the absence of isobutanol are relevant to branched-chain alcohol tolerance (Figure S7B).

Comparing the transcriptomes of the wild-type and *gln3Δ* strains in the presence of isobutanol reveals meaningful differences in their cellular responses. When grown in isobutanol, there are 234 genes significantly upregulated or downregulated in the *gln3Δ* strain relative to the wild-type strain (Figure 5B; Tables S7G and S7H). The most remarkable difference is that the largest group of genes downregulated in the *gln3Δ* strain relative to the wild-type strain is involved in amino acid biosynthesis (Figures 5B and S6A; Table S7H), with additional downregulated genes involved in cellular import of amino acids (Table S7H). Given the role of *GLN3* in the regulation of genes controlled by nitrogen catabolite repression, this effect is not intrinsically surprising. However, this result is more meaningful in light of

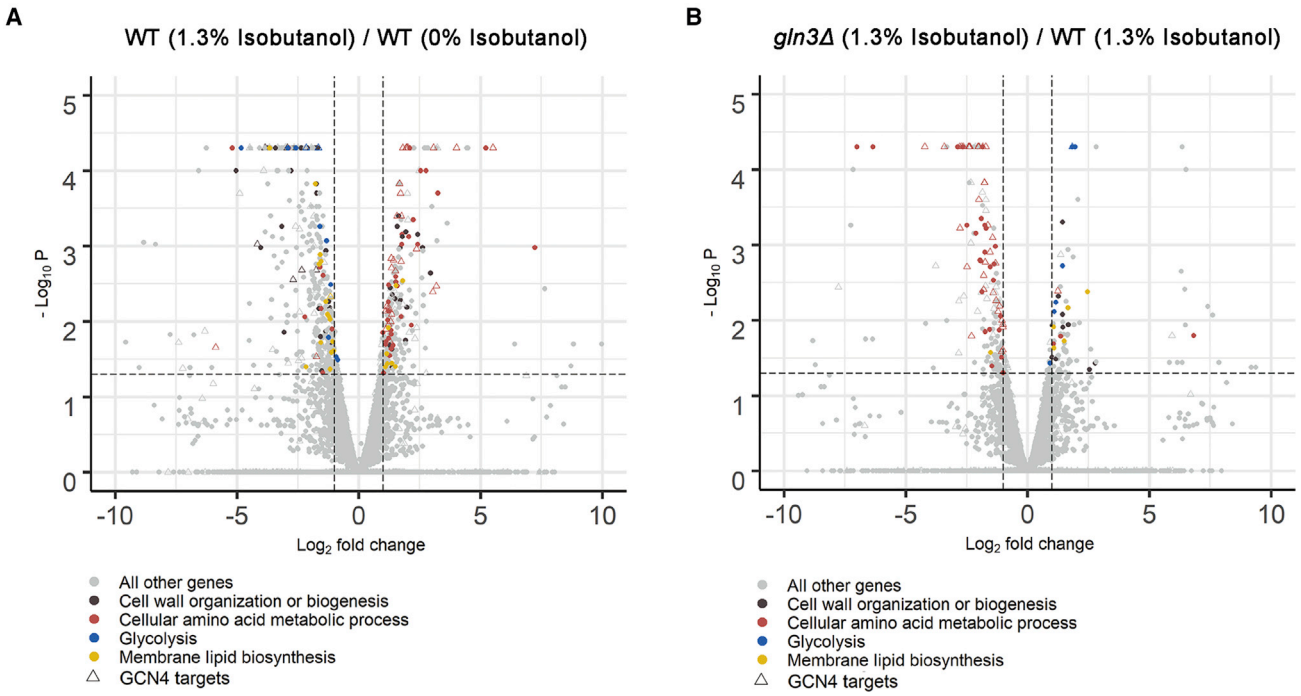

Figure 5. Volcano Plots Representing Differentially Expressed Genes

(A) Comparison of the transcriptomic profiles of the wild-type strain grown with 1.3% (v/v) isobutanol and the wild-type strain grown without isobutanol.

(B) Comparison of the transcriptomic profiles of the *gln3Δ* strain grown with 1.3% (v/v) isobutanol and the wild-type strain grown with 1.3% (v/v) isobutanol. Each point represents one gene whose position is determined by the average $\log_2$ fold change and negative $\log_{10}$ p value from two independent experiments. Dashed lines indicate cutoffs where $|\text{Log}_2 \text{ fold change}| > 1$ and p value < 0.05. Among genes differentially expressed, genes regulated by Gcn4p are labeled as triangles. See also Figures S6 and S7; Tables S6 and S7.

the fact that these genes are strongly induced in the wild-type strain in response to isobutanol (Figures 5A and S6A; Table S7A).

Several genes involved in processes essential for cell division are upregulated in the *gln3Δ* strain relative to the wild type when they are both grown in isobutanol (Figure 5B; Table S7G). These include genes involved in glycolysis (*TDH1*, *TDH2*, *ENO1*, *ENO2*, *CDC19*, and *GPM1*), cell wall organization or biogenesis (as defined by the GO term in Table S7), and membrane lipid biosynthesis (listed in the legend of Figure S7). The differences in expression of glycolytic genes stem from the repression of these genes in the wild-type strain in the presence of isobutanol (Figure 5A; Table S7B), rather than induction of these genes by isobutanol in the *gln3Δ* strain (Table S7C). In fact, the glycolytic gene *TDH1* is even slightly repressed in the *gln3Δ* strain in the presence of isobutanol (Table S7D). In contrast, the origin of differences in expression of genes involved in cell wall or membrane lipid biosynthesis is more complex (Table S7). Although the cell wall is typically known for providing structure to the cell, proteins on the exterior of the cell wall also influence its permeability (Klis et al., 2002). In addition, the protein composition of the cell wall is dynamic, responding to the extracellular environment (Klis et al., 2002). Thus, upregulation of genes encoding cell wall proteins (e.g., *CIS3*, *DAN1*, *SCW4*, and *SRL1*) may contribute to increased tolerance of the *gln3Δ* strain by reducing the permeability of the cell wall to isobutanol. In a similar manner, genes involved in the biosynthesis and regulation of phospholipids and sterols are crucial in determining the properties of the plasma membrane and its ability to tolerate extracellular stress (Kodedová and Sychrová, 2015). The upregulation of genes involved in phospholipid (*INO1*, *OPI3*, and *PLB2*) and ergosterol (*HES1*) biosynthesis (Table S7G) raises the possibility that the composition of the plasma membrane is altered in the *gln3Δ* strain in the presence of isobutanol. *FAS1*, required for long-chain fatty acid synthesis, and therefore important in membrane biosynthesis, is also upregulated in *gln3Δ* strain compared to the wild-type strain in the presence of isobutanol (Table S7G); notably, its expression is unaltered in all of our other transcriptomic comparisons (Tables S7A–S7F). Together, these results suggest that in the presence of isobutanol, the wild-type strain is largely devoted to scavenging for nitrogen sources and synthesizing amino acids at the expense of glycolysis, as well as cell wall and membrane biosynthesis and integrity, which are important for cell division and likely tolerance. On the other hand, the *gln3Δ* strain is unable to mount the same nitrogen starvation response, which helps it maintain closer to normal levels of glycolysis as well as cell wall and membrane maintenance, consistent with it having better growth and tolerance in isobutanol than the wild-type strain.

Isobutanol Impacts the Intracellular Levels of Glutamine and Glutamate

Given the role of *GLN3* in glutamine biosynthesis, (Mitchell and Magasanik, 1984) and the relationship between glutamine and glutamate, we expected to find significant differences in the intracellular concentrations of these two amino acids when comparing

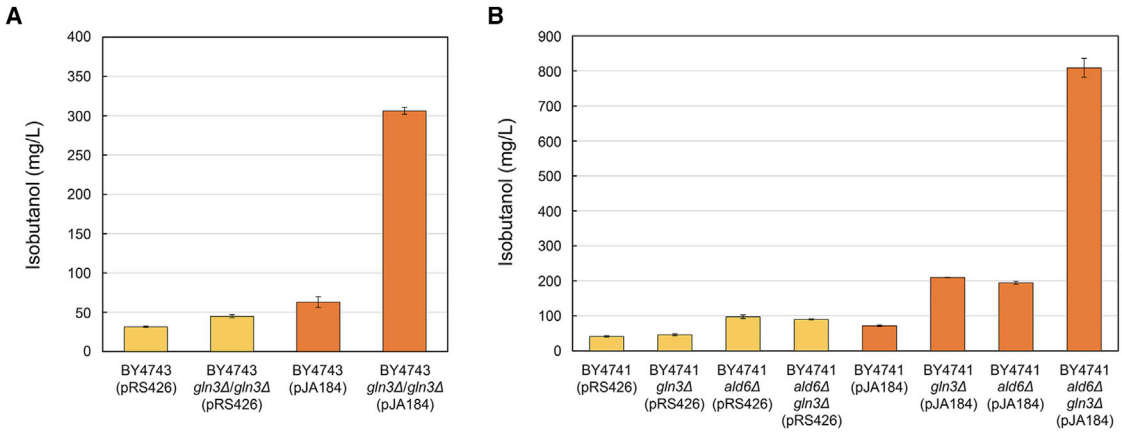

Figure 6. Isobutanol Production by Isobutanol-Tolerant Strains with *GLN3* Deletions

(A) Isobutanol production of the *gln3Δ/gln3Δ* homozygous diploid BY4743 strain as compared to wild-type BY4743, harboring a 2 μ plasmid with the isobutanol pathway (pJA184). Error bars represent the SEM of three independent experiments.

(B) Effects of *GLN3* and *ALD6* deletions on isobutanol production of the haploid BY4741 strain. Error bars represent the SEM of three independent experiments. Yellow bars indicate that the strain harbors an empty 2 μ plasmid (pRS426) and orange bars indicate that the strain harbors the 2 μ plasmid, pJA184. These experiments were carried out in commercial medium, but the effect also occurs in medium prepared in-house (Figure S10).

the *gln3Δ* and wild-type strains grown with isobutanol. To test this hypothesis, we measured the intracellular concentrations of glutamine and glutamate in the wild type and *gln3Δ* strains grown with or without isobutanol. We found that the *gln3Δ* strain has lower glutamine (Figure S8A) but higher glutamate (Figure S8B) intracellular concentrations than the wild-type strain in the presence or absence of isobutanol, consistent with reduced expression of *GLN1* in the *gln3Δ* strain compared to the wild type, regardless of the presence of isobutanol (Figure S6A; Tables S7F and S7H). However, in both the wild type and *gln3Δ* strains, isobutanol causes an increase in intracellular concentrations of both glutamine and glutamate, suggesting the existence of mechanisms independent of *GLN3* that still elevate intracellular amino acid concentrations in response to isobutanol. The significant changes in intracellular concentrations and proportions of glutamine and glutamate in response to deletion of *GLN3* and isobutanol stress may influence cell sensitivity and tolerance to branched-chained alcohols.

Branched-Chain Alcohols Induce Morphological Changes in the *gln3Δ* Strain

To study the effect of the *GLN3* deletion on cell morphology, we examined cell size and shape of the wild type and *gln3Δ* strains with or without three different alcohols. We found that branched-chain alcohols (isobutanol and tert-butanol) induce a filamentous-like phenotype in the *gln3Δ* strain but not in the wild type (Figure S9). However, the linear alcohol 1-butanol does not induce this morphological change in wild type or *gln3Δ* strains. Alcohols are known to induce filamentation in yeast (Lorenz et al., 2000); however, the BY4741 parental strain has a filamentation defect because of a mutation in *FLO8*, which is a positive regulator of this process (Liu et al., 1996; Lorenz et al., 2000). Based on our observations, the *GLN3* deletion seems to partially suppress this defect by a mechanism that we have not yet identified.

Our RNA-seq data suggest that filamentation may play a role in the specific tolerance of the *gln3Δ* strain to branched-chain alcohols. *KDX1*, encoding a kinase and mitogen-activated protein kinase (MAPK) pathway component (Breitkreutz et al., 2010), is significantly upregulated when the *gln3Δ* strain is grown in isobutanol compared to the wild type grown in the same conditions. *KDX1* upregulates *RCK1*, a gene known to be involved in pseudo-hyphal formation (Chang et al., 2013, 2014). Previous genome-wide overexpression screens have also directly linked *KDX1* to invasive filamentation (Shively et al., 2013).

Isobutanol Production Is Markedly Increased in the Hypertolerant *gln3Δ* Strain

We hypothesized that enhancing isobutanol tolerance in a strain engineered to produce it could boost production. To test this possibility, we overexpressed five genes in the isobutanol biosynthetic pathway, *ILV2*, *ILV3*, *ILV5*, and *ADH7* from *S. cerevisiae* and 2-ketoacid decarboxylase (KDC) from *Lactococcus lactis* in the *gln3Δ* strain in their native locations (mitochondria and cytosol) or targeted exclusively to the mitochondria, which considerably increases isobutanol titers (Avalos et al., 2013). We introduced the native or mitochondrial isobutanol biosynthetic pathways into a *gln3Δ/gln3Δ* homozygous diploid BY4743 strain using a 2 μ plasmid and compared isobutanol production to equivalent strains constructed in the wild-type background. Homozygous deletion of *GLN3* and overexpression of the isobutanol biosynthetic enzymes in their native locations (mitochondria and cytosol) using constitutive promoters (pJA184) enhances isobutanol production 4.9-fold relative to BY4743 harboring the same plasmid (pJA184), from 63 ± 7 mg/L in the wild type to 306 ± 4 mg/L (Figure 6A). Deletion of *GLN3* enhances isobutanol production in engineered BY4743 strains in both commercial (Figure 6A) and in-house prepared (Figure S10) media (Table S8). While isobutanol titers did not improve in strains harboring the mitochondrial pathway (data not shown), the effect of the *GLN3* deletion is preserved in haploid strains overexpressing the natively localized isobutanol pathway. The BY4741 *gln3Δ* strain harboring pJA184 exhibits a 2.9-fold increase in titers compared to the wild-type BY4741 harboring the same plasmid (Figure 6B). Additional deletion of *ALD6*, which boosts isobutanol titers (Park et al., 2014), acts synergistically with the *GLN3* deletion

to further increase isobutanol production. The *ald6Δ gln3Δ* strain harboring pJA184 achieves an isobutanol titer of 809 ± 27 mg/L, representing a 4.1-fold improvement over the *ald6Δ* strain and an 11.3-fold increase in isobutanol production over the wild-type strain harboring the same plasmid (Figure 6B). These results suggest that enhancing isobutanol tolerance by deleting *GLN3* is a useful strategy for improving isobutanol titers in engineered yeast strains.

DISCUSSION

Enhancement of branched-chain alcohol production in yeast requires not only increasing productivity but also improving yeast tolerance to their toxic effects. In this study, we screened the yeast deletion library for isobutanol tolerance and sensitivity. The only previous study investigating isobutanol toxicity in yeast used RNAi libraries to screen for strains with enhanced tolerance to isobutanol or 1-butanol (Crook et al., 2016). By contrast, our study provides genomic-scale, quantitative information on how each non-essential gene in the yeast genome affects isobutanol tolerance.

Our screens revealed that some genes, such as those involved in tryptophan biosynthesis and vacuolar function, are important for general cell tolerance to both simple alcohols (methanol, ethanol) and higher alcohols. We found that deletions of *TRP1–5*, involved in tryptophan biosynthesis increase the sensitivity of yeast to alcohols (Table S3). Deletion of *TRP1* has also been shown to increase yeast sensitivity to DNA damaging agents (Godin et al., 2016) and metal ions (González et al., 2008). Furthermore, deletion of any one of the *TRP1–5* genes increases sensitivity to ethanol, rapamycin, high pH, and sodium dodecyl sulfate (González et al., 2008; Hirasawa et al., 2007). Thus, it is advisable to avoid strains containing the *trp1Δ* auxotrophic marker when producing alcohols as their inherent hypersensitivity to these products could limit titers.

Our screens also revealed that genes encoding enzymes in the PPP are important for tolerance specifically to isobutanol and other higher alcohols (C4–C6), without influencing tolerance to ethanol. The PPP is critical in maintaining cellular redox homeostasis by reducing $NADP^+$ to NADPH, which is generally accepted to provide reducing energy for enzymes involved in stress responses. Among the studies demonstrating that deletion of PPP genes decreases yeast tolerance to furfural, acetaldehyde, and oxidative stress (Gorsich et al., 2006; Juhnke et al., 1996; Krüger et al., 2011; Matsufuji et al., 2008), several suggest that the cause of reduced tolerance is the decrease in intracellular levels of NADPH. However, none of them report measurements of intracellular NADPH. Here, we show that deleting PPP genes encoding enzymes that catalyze NADPH-generating reactions does not necessarily cause decreased ratios of NADPH/$NADP^+$ (Figure S4). The *gnd1Δ* strain, which we found to be the most isobutanol-sensitive strain, has an NADPH/$NADP^+$ ratio in the presence of isobutanol at least as high as that of the wild type. This implies that the role of the PPP in yeast tolerance to higher alcohols cannot be limited to the provision of high NADPH/$NADP^+$ ratios to enzymes involved in the stress response. Our results are consistent with the previous observation that NADPH availability does not fully account for the sensitivity of PPP deletion strains to oxidative stress, and that PPP genes are important for inducing transcriptional responses to oxidative stress (Krüger et al., 2011).

Our genomic screens for hypertolerance revealed that deletion of *GLN3* is the single most impactful deletion for enhancing yeast tolerance to isobutanol (Figure 4A). The fact that the enhanced tolerance of the *gln3Δ* strain is specific to branched-chain alcohols, having no effect on tolerance to ethanol or higher linear alcohols (Figure 4B), suggests that the toxicity caused by isobutanol and other branched-chain alcohols has a unique mechanism of action, and that branched-chain alcohols induce a specific adaptive response in yeast. Our transcriptomic study sheds light on the specific mechanisms by which branched-chain alcohols induce toxicity, and how deletion of *GLN3* makes cells less sensitive.

When nitrogen sources are scarce, yeast resort to utilizing their own amino acids as a nitrogen source, including branched-chain amino acids (Rødkaer and Faergeman, 2014). This process involves the Ehrlich degradation pathway, which converts valine, leucine, and isoleucine to isobutanol, isopentanol, and 2-methyl-1-butanol, respectively, after they have been deaminated (Hazelwood et al., 2008). Therefore, yeast has evolved to sense these fusel alcohols as a signal for nitrogen starvation (Ashe et al., 2001). Consistent with this adaptive trait, when the wild-type strain is grown in the presence of isobutanol, our transcriptomic data show that the cells respond as if they were starving for nitrogen, even though they are growing in medium rich with amino acids and ammonium sulfate (Table S8). The isobutanol-induced nitrogen starvation response we observe is two-pronged: (1) the cell induces many genes involved in amino acid biosynthesis and transport of nitrogen sources, including amino acids (Figure 5A; Table S7A); (2) the cell represses glycolysis, and genes involved in cell wall biogenesis and membrane lipid biosynthesis (Figure 5A; Table S7B). Our hypothesis that isobutanol induces a nitrogen starvation response, resulting in reduced transcription of glycolytic genes (Figures 7A and 7B) is consistent with the observation that the vacuolar proteinase Pep4p is downregulated in wild-type cells grown with isobutanol (Table S7B). Deletion of Pep4p under nitrogen starvation conditions reduces both transcription and post-translational modification of glycolytic enzymes (Hu et al., 2019).

This natural response is appropriate when cells are truly starving for nitrogen and exposed to sub-lethal isobutanol concentrations, as evolution would favor cells that stop dividing and shift their metabolism to prioritize amino acid biosynthesis and nitrogen conservation and assimilation. However, in fermentations designed to produce isobutanol, the natural nitrogen starvation response is counterproductive. Not only do the cells waste energy and resources producing and scavenging for amino acids they do not need, but they also take these resources away from processes necessary to divide and withstand high isobutanol concentrations.

This mechanism of isobutanol toxicity is consistent with our finding that deletion of *GLN3* significantly enhances yeast tolerance to branched-chain alcohols. *GLN3* encodes a transcription factor that activates several genes that are repressed when cells have access to high-quality nitrogen sources, such as glutamine, asparagine, or ammonia (Scherens et al., 2006). Under such conditions, Gln3p is phosphorylated and sequestered in the cytosol by Ure2p, which prevents Gln3p from activating its target genes (Conrad et al., 2014). When the cell has access to only low quality

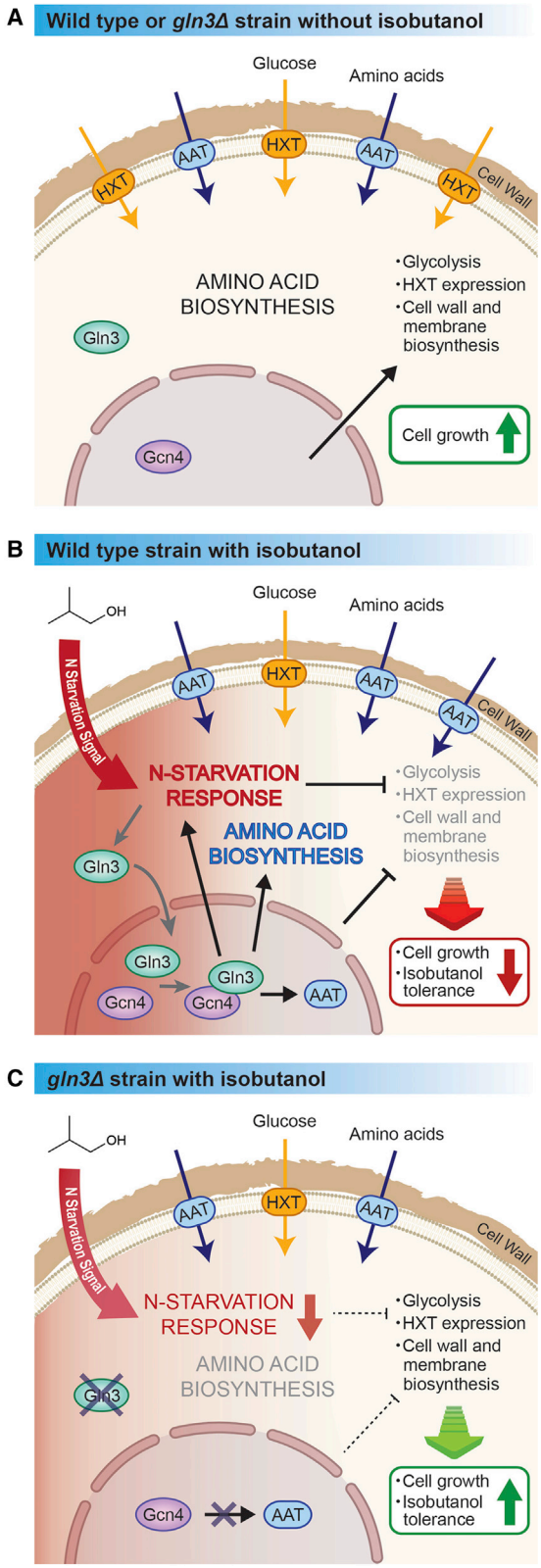

Figure 7. Schematic Model of the Proposed Response Mechanism to Isobutanol Stress in Wild-Type and *GLN3* Deletion Strains

(A) Behavior of wild-type or *gln3Δ* strains grown in nitrogen-rich conditions without isobutanol in the media. Glucose and amino acids are imported into the cell via hexose transporters (HXT) and amino acid transporters (AAT), respectively. Glycolysis, cell wall biogenesis, and membrane lipid biosynthesis are prioritized.

(B) Natural response of wild-type cells to extracellular isobutanol stress. Isobutanol triggers a nitrogen starvation response, causing the transcription factor Gln3p to enter the nucleus. Gln3p forms a complex with transcription factor Gcn4p, which together activate transcription of genes involved in amino acid biosynthesis and import. Gln3p may also strengthen the nitrogen starvation response, causing downregulation of glycolytic genes, and genes involved hexose import, cell wall biogenesis, and membrane lipid biosynthesis. As a result, cell growth and the cell's ability to tolerate isobutanol stress are repressed.

(C) Deletion of *GLN3* evades the natural nitrogen starvation response to enhance tolerance and growth in isobutanol. Without *GLN3*, genes involved in glycolysis, cell wall biogenesis, and membrane lipid biosynthesis are upregulated, while those involved in amino acid biosynthesis and import are downregulated compared to the wild-type strain grown in the same conditions. As a result, cell growth and the ability to tolerate isobutanol stress are more active. Expression of HXT genes is unchanged between the wild-type and *gln3Δ* strains grown with isobutanol. See also Figures 5, S6, and S7; Tables S6 and S7.

nitrogen sources, such as proline or urea, or senses nitrogen starvation, the Tor1p-containing TOR Complex 1 (TORC1) releases its repression over the Tap42-Sit4 and Tap42-PP2A complexes, which in turn dephosphorylate Gln3p, allowing it to dissociate from Ure2p, enter the nucleus, and initiate the nitrogen starvation response (Conrad et al., 2014). Thus, when *GLN3* is deleted, this signaling pathway is interrupted, and the nitrogen starvation response fails to implement. As a result, the *gln3Δ* strain does not waste resources needlessly synthesizing amino acids or scavenging for nitrogen; it instead keeps glycolysis active, affording the cell more energy to affront isobutanol toxicity, as well as other processes required for cell division (Figure 7C). This mechanism is also consistent with the observation that deletion of *GLN3* enhances tolerance to branched-chain alcohols, but not to linear or simple alcohols, as only the former would be recognized as degradation products of amino acids, initiating a nitrogen starvation signal to which *GLN3* has evolved to respond.

Our genomic and transcriptomic data suggest that isobutanol activates *GCN4*, allowing Gln3p to induce its target genes. Deletion of *GCN4*, or its activator *GCN3*, result in strains with enhanced tolerance to 1.4% isobutanol – with tolerance factors of 0.86 and 0.98, respectively, compared to a tolerance factor of 0.38 for the wild type (Tables S1 and S2)—consistent with the role of Gcn4p in keeping Gln3p in the nucleus during nitrogen starvation (Tate et al., 2017). Furthermore, multiple genes regulated by *GCN4* are downregulated in the *gln3Δ* strain grown with isobutanol compared to the wild-type strain with isobutanol (Figure 5B). Although *GLN3* is not directly transcriptionally regulated by Gcn4p (Sosa et al., 2003), it has been shown that a Gln3-Gcn4 protein complex forms in response to nitrogen starvation, which focuses the transcriptional response of Gcn4p to genes regulated by Gln3p (Hernández et al., 2011). Our results suggest that the genes regulated by Gcn4p that are differentially expressed in the wild-type and *gln3Δ* strains in the presence of isobutanol (Figure 5B; Table S7H) are controlled by this Gln3-Gcn4

protein complex, expanding the list of known genes regulated by *GLN3* and offering an additional explanation for the enhanced isobutanol tolerance of the *gcn4Δ* strain.

Our measurements of intracellular amino acid concentrations also support a mechanism wherein the enhanced isobutanol tolerance of *gln3Δ* strains is linked to amino acid metabolism. *GLN3* regulates intracellular levels of glutamine and glutamate, which serve as nitrogen donors, and are typically the amino acids with the highest intracellular concentrations (Mülleder et al., 2016). *GLN1*, a target gene of Gln3p, encodes an enzyme involved in biosynthesis of glutamine from glutamate (Crespo et al., 2002). Consistent with its regulation by Gln3p, *GLN1* is downregulated in the *gln3Δ* strain relative to the wild type in both the absence and presence of isobutanol (Tables S7F and S7H). Furthermore, previous results showed that inhibition of *GLN1* causes depletion of intracellular glutamine (Crespo et al., 2002). Thus, it is likely that downregulation of *GLN1* is the cause of the decreases in intracellular glutamine levels and increases in intracellular glutamate levels we observe upon the deletion of *GLN3* in both media conditions (Figures S8A and S8B).

The adaptive response of yeast to isobutanol, which the cell recognizes as a signal of nitrogen starvation, causes toxicity by inhibiting cell growth even before isobutanol inflicts physical damage to the cell. For this reason, disruption of this response by deleting *GLN3* leads to a 4.04-fold increase in isobutanol tolerance compared to the wild type (Figure 4B). Furthermore, disruption of this adaptive mechanism can markedly boost isobutanol titers in strains engineered to produce it (Figure 6). However, it is not clear why this approach works only when the enzymes for isobutanol biosynthesis are localized in their natural compartments. It is possible that tampering with mitochondria to make isobutanol evades the natural starvation response to isobutanol, such that the mitochondrial pathway fails to benefit from deleting *GLN3*. Future studies will be needed to determine the reasons why the *GLN3* deletion does not enhance isobutanol production in strains harboring the mitochondrial isobutanol pathway.

Our findings provide insights into the cellular response of yeast to isobutanol, and mechanisms underlying specific toxicity and tolerance to isobutanol and other branched-chain alcohols (Figure 7). Strains identified or engineered for their enhanced tolerance to specific chemicals do not necessarily result in increased production of those chemicals (Atsumi et al., 2010; Foo et al., 2014). In fact, no previous work has demonstrated that isobutanol production can be improved by addressing product toxicity. Thus, we establish the basis for constructing robust yeast strains with enhanced tolerance to isobutanol, resulting in increased isobutanol production. Overall, this work sheds light on a basic mechanism of isobutanol toxicity, the adaptive response of yeast to branched-chain alcohols, and a promising strategy to boost isobutanol production by genetically disrupting this response.

STAR★METHODS

Detailed methods are provided in the online version of this paper and include the following:

SUPPLEMENTAL INFORMATION

Supplemental Information can be found online at https://doi.org/10.1016/j.cels.2019.10.006.

ACKNOWLEDGMENTS

This work was supported by the US Department of Energy, Office of Science, Office of Biological and Environmental Research, Genomic Science Program under award number DESC0019363 (to J.L.A.), as well as the NSF CAREER award 1751840, the Pew Charitable Trusts, the Alfred P. Sloan Foundation, and the Yang Family Foundation for Engineering from Princeton University SEAS (to J.L.A.); the John Mung Program Kyoto University (to K.K.); the SPIRITS 2017 of Kyoto University (to K.K. and M.U.); the NSF Graduate Research Fellowship Program grant DGE-1656466 (to S.K.H.); NIH grant GM035010 (to G.R.F.); and DOE grant 6935036 (to G.S.).

AUTHOR CONTRIBUTIONS

K.K., G.R.F., and J.L.A. conceived the project and designed the experiments. S.K.H. conducted isobutanol production experiments and NADPH/NADP$^+$ ratio measurements. Y.W. carried out RNA-seq analysis and quantification of intracellular amino acids. J.M.L. analyzed RNA-seq data and prepared the volcano plots. K.K. performed isobutanol production in the in-house-prepared medium and all other experiments. K.K., S.K.H., G.R.F., and J.L.A. analyzed the results. K.K., G.R.F., G.S., M.U., and J.L.A. allocated materials and resources. K.K. and J.L.A. supervised the project. K.K., S.K.H., and J.L.A. wrote the manuscript in consultation with G.R.F., G.S., and M.U.

DECLARATION OF INTERESTS

The authors declare no competing interests. A patent application describing the isobutanol hypertolerant mutants is currently pending.

Received: December 26, 2018
Revised: August 23, 2019
Accepted: October 18, 2019
Published: November 13, 2019

REFERENCES

Ashe, M.P., Slaven, J.W., De Long, S.K., Ibrahimo, S., and Sachs, A.B. (2001). A novel eIF2B-dependent mechanism of translational control in yeast as a response to fusel alcohols. EMBO J. *20*, 6464–6474.

Atsumi, S., Wu, T.Y., Machado, I.M., Huang, W.C., Chen, P.Y., Pellegrini, M., and Liao, J.C. (2010). Evolution, genomic analysis, and reconstruction of isobutanol tolerance in *Escherichia coli*. Mol. Syst. Biol. *6*, 449.

Avalos, J.L., Fink, G.R., and Stephanopoulos, G. (2013). Compartmentalization of metabolic pathways in yeast mitochondria improves the production of branched-chain alcohols. Nat. Biotechnol. *31*, 335–341.

Boyle, E.I., Weng, S., Gollub, J., Jin, H., Botstein, D., Cherry, J.M., and Sherlock, G. (2004). GO::TermFinder–open source software for accessing Gene Ontology information and finding significantly enriched Gene Ontology terms associated with a list of genes. Bioinformatics *20*, 3710–3715.

Brachmann, C.B., Davies, A., Cost, G.J., Caputo, E., Li, J., Hieter, P., and Boeke, J.D. (1998). Designer deletion strains derived from *Saccharomyces cerevisiae* S288C: a useful set of strains and plasmids for PCR-mediated gene disruption and other applications. Yeast *14*, 115–132.

Bramucci, M.G., Larossa, R.A., and Singh, M. (2013). Yeast with increased butanol tolerance involving filamentous growth response (Butamax Advanced Biofuels LLC).

Brat, D., Weber, C., Lorenzen, W., Bode, H.B., and Boles, E. (2012). Cytosolic re-localization and optimization of valine synthesis and catabolism enables increased isobutanol production with the yeast *Saccharomyces cerevisiae*. Biotechnol. Biofuels *5*, 65.

Breitkreutz, A., Choi, H., Sharom, J.R., Boucher, L., Neduva, V., Larsen, B., Lin, Z.Y., Breitkreutz, B.J., Stark, C., Liu, G., et al. (2010). A global protein kinase and phosphatase interaction network in yeast. Science *328*, 1043–1046.

Brooks, K.P., Snowden-Swan, L.J., Jones, S.B., Butcher, M.G., Lee, G.S.J., Anderson, D.M., Frye, J.G., Holladay, J.E., Owen, J., Harmon, L., et al. (2016). Low-carbon aviation fuel through the alcohol to jet pathway. In Biofuels for aviation, C.J. Chuck, ed. (Academic Press), pp. 109–150.

Chang, M., Kang, H.J., Baek, I.J., Kang, C.M., Park, Y.S., and Yun, C.W. (2013). Kdx1 regulates RCK1 gene expression by interacting with Rlm1 in Saccharomyces cerevisiae. Biochem. Biophys. Res. Commun. *435*, 350–355.

Chang, M., Kang, C.M., Park, Y.S., and Yun, C.W. (2014). Rck1 up-regulates pseudohyphal growth by activating the Ras2 and MAP kinase pathways independently in *Saccharomyces cerevisiae*. Biochem. Biophys. Res. Commun. *444*, 656–661.

Chen, Y., Wang, Y., Chen, T.H., Yao, M.D., Xiao, W.H., Li, B.Z., and Yuan, Y.J. (2018). Identification and manipulation of a novel locus to improve cell tolerance to short-chain alcohols in *Escherichia coli*. J. Ind. Microbiol. Biotechnol. *45*, 589–598.

Chomczynski, P., and Sacchi, N. (2006). The single-step method of RNA isolation by acid guanidinium thiocyanate-phenol-chloroform extraction: twenty-something years on. Nat. Protoc. *1*, 581–585.

Christianson, T.W., Sikorski, R.S., Dante, M., Shero, J.H., and Hieter, P. (1992). Multifunctional yeast high-copy-number shuttle vectors. Gene *110*, 119–122.

Conrad, M., Schothorst, J., Kankipati, H.N., Van Zeebroeck, G., Rubio-Texeira, M., and Thevelein, J.M. (2014). Nutrient sensing and signaling in the yeast *Saccharomyces cerevisiae*. FEMS Microbiol. Rev. *38*, 254–299.

Courchesne, W.E., and Magasanik, B. (1988). Regulation of nitrogen assimilation in *Saccharomyces cerevisiae*: roles of the *URE2* and *GLN3* genes. J. Bacteriol. *170*, 708–713.

Crespo, J.L., Powers, T., Fowler, B., and Hall, M.N. (2002). The TOR-controlled transcription activators GLN3, RTG1, and RTG3 are regulated in response to intracellular levels of glutamine. Proc. Natl. Acad. Sci. USA *99*, 6784–6789.

Crook, N., Sun, J., Morse, N., Schmitz, A., and Alper, H.S. (2016). Identification of gene knockdown targets conferring enhanced isobutanol and 1-butanol tolerance to *Saccharomyces cerevisiae* using a tunable RNAi screening approach. Appl. Microbiol. Biotechnol. *100*, 10005–10018.

Dunlop, M.J. (2011). Engineering microbes for tolerance to next-generation biofuels. Biotechnol. Biofuels *4*, 32.

Dürre, P. (2007). Biobutanol: an attractive biofuel. Biotechnol. J. *2*, 1525–1534.

Eisen, M.B., Spellman, P.T., Brown, P.O., and Botstein, D. (1998). Cluster analysis and display of genome-wide expression patterns. Proc. Natl. Acad. Sci. USA *95*, 14863–14868.

Entian, K.D., and Kötter, P. (2007). 25 Yeast genetic strain and plasmid collections. Methods Microbiol. *36*, 629–666.

Foo, J.L., Jensen, H.M., Dahl, R.H., George, K., Keasling, J.D., Lee, T.S., Leong, S., and Mukhopadhyay, A. (2014). Improving microbial biogasoline production in *Escherichia coli* using tolerance engineering. mBio *5*, e01932.

Fujita, K., Matsuyama, A., Kobayashi, Y., and Iwahashi, H. (2006). The genome-wide screening of yeast deletion mutants to identify the genes required for tolerance to ethanol and other alcohols. FEMS Yeast Res. *6*, 744–750.

Ghiaci, P., Norbeck, J., and Larsson, C. (2013). Physiological adaptations of *Saccharomyces cerevisiae* evolved for improved butanol tolerance. Biotechnol. Biofuels *6*, 101.

Giaever, G., Chu, A.M., Ni, L., Connelly, C., Riles, L., Véronneau, S., Dow, S., Lucau-Danila, A., Anderson, K., André, B., et al. (2002). Functional profiling of the *Saccharomyces cerevisiae* genome. Nature *418*, 387–391.

Godin, S.K., Lee, A.G., Baird, J.M., Herken, B.W., and Bernstein, K.A. (2016). Tryptophan biosynthesis is important for resistance to replicative stress in *Saccharomyces cerevisiae*. Yeast *33*, 183–189.

González, A., Larroy, C., Biosca, J.A., and Ariño, J. (2008). Use of the *TRP1* auxotrophic marker for gene disruption and phenotypic analysis in yeast: a note of warning. FEMS Yeast Res. *8*, 2–5.

González-Ramos, D., van den Broek, M., van Maris, A.J., Pronk, J.T., and Daran, J.M. (2013). Genome-scale analyses of butanol tolerance in *Saccharomyces cerevisiae* reveal an essential role of protein degradation. Biotechnol. Biofuels *6*, 48.

Gorsich, S.W., Dien, B.S., Nichols, N.N., Slininger, P.J., Liu, Z.L., and Skory, C.D. (2006). Tolerance to furfural-induced stress is associated with pentose phosphate pathway genes *ZWF1*, *GND1*, *RPE1*, and *TKL1* in *Saccharomyces cerevisiae*. Appl. Microbiol. Biotechnol. *71*, 339–349.

Gueldener, U., Heinisch, J., Koehler, G.J., Voss, D., and Hegemann, J.H. (2002). A second set of loxP marker cassettes for Cre-mediated multiple gene knockouts in budding yeast. Nucleic Acids Res. *30*, e23.

Hammer, S.K., and Avalos, J.L. (2017). Uncovering the role of branched-chain amino acid transaminases in *Saccharomyces cerevisiae* isobutanol biosynthesis. Metab. Eng. *44*, 302–312.

Hazelwood, L.A., Daran, J.M., van Maris, A.J., Pronk, J.T., and Dickinson, J.R. (2008). The Ehrlich pathway for fusel alcohol production: a century of research on *Saccharomyces cerevisiae* metabolism. Appl. Environ. Microbiol. *74*, 2259–2266.

Hernández, H., Aranda, C., Riego, L., and González, A. (2011). Gln3-Gcn4 hybrid transcriptional activator determines catabolic and biosynthetic gene expression in the yeast *Saccharomyces cerevisiae*. Biochem. Biophys. Res. Commun. *404*, 859–864.

Hirasawa, T., Yoshikawa, K., Nakakura, Y., Nagahisa, K., Furusawa, C., Katakura, Y., Shimizu, H., and Shioya, S. (2007). Identification of target genes conferring ethanol stress tolerance to *Saccharomyces cerevisiae* based on DNA microarray data analysis. J. Biotechnol. *131*, 34–44.

Hu, J., Yu, L., Shu, Q., and Chen, Q. (2019). Identification of down-regulated proteome in *Saccharomyces cerevisiae* with the deletion of yeast cathepsin D in response to nitrogen stress. Microorganisms *7*, E214.

Huang, Z., Chen, K., Zhang, J., Li, Y., Wang, H., Cui, D., Tang, J., Liu, Y., Shi, X., Li, W., et al. (2013). A functional variomics tool for discovering drug-resistance genes and drug targets. Cell Rep. *3*, 577–585.

Huffer, S., Clark, M.E., Ning, J.C., Blanch, H.W., and Clark, D.S. (2011). Role of alcohols in growth, lipid composition, and membrane fluidity of yeasts, bacteria, and archaea. Appl. Environ. Microbiol. *77*, 6400–6408.

Ito, H., Fukuda, Y., Murata, K., and Kimura, A. (1983). Transformation of intact yeast cells treated with alkali cations. J. Bacteriol. *153*, 163–168.

Juhnke, H., Krems, B., Kötter, P., and Entian, K.D. (1996). Mutants that show increased sensitivity to hydrogen peroxide reveal an important role for the pentose phosphate pathway in protection of yeast against oxidative stress. Mol. Gen. Genet. *252*, 456–464.

Kern, S.E., Price-Whelan, A., and Newman, D.K. (2014). Extraction and measurement of $NAD(P)^+$ and NAD(P)H. Methods Mol. Biol. *1149*, 311–323.

Klis, F.M., Mol, P., Hellingwerf, K., and Brul, S. (2002). Dynamics of cell wall structure in *Saccharomyces cerevisiae*. FEMS Microbiol. Rev. *26*, 239–256.

Knoshaug, E.P., and Zhang, M. (2009). Butanol tolerance in a selection of microorganisms. Appl. Biochem. Biotechnol. *153*, 13–20.

Kodedová, M., and Sychrová, H. (2015). Changes in the sterol composition of the plasma membrane affect membrane potential, salt tolerance and the activity of multidrug resistance pumps in *Saccharomyces cerevisiae*. PLoS One *10*, e0139306.

Krüger, A., Grüning, N.M., Wamelink, M.M., Kerick, M., Kirpy, A., Parkhomchuk, D., Bluemlein, K., Schweiger, M.R., Soldatov, A., Lehrach, H., et al. (2011). The pentose phosphate pathway is a metabolic redox sensor and regulates transcription during the antioxidant response. Antioxid. Redox Signal. *15*, 311–324.

Kubota, S., Takeo, I., Kume, K., Kanai, M., Shitamukai, A., Mizunuma, M., Miyakawa, T., Shimoi, H., Iefuji, H., and Hirata, D. (2004). Effect of ethanol on cell growth of budding yeast: genes that are important for cell growth in the presence of ethanol. Biosci. Biotechnol. Biochem. *68*, 968–972.

Kuroda, K., and Ueda, M. (2016). Cellular and molecular engineering of yeast *Saccharomyces cerevisiae* for advanced biobutanol production. FEMS Microbiol. Lett. *363*.

Lam, F.H., Ghaderi, A., Fink, G.R., and Stephanopoulos, G. (2014). Biofuels. Engineering alcohol tolerance in yeast. Science *346*, 71–75.

LaRossa, R.A. (2013). Yeast strain for production of four carbon alcohols (Butamax Advanced Biofuels LLC).

Leão, C., and van Uden, N. (1982). Effects of ethanol and other alkanols on the glucose transport system of *Saccharomyces cerevisiae*. Biotechnol. Bioeng. *24*, 2601–2604.

Liu, S., and Qureshi, N. (2009). How microbes tolerate ethanol and butanol. New Biotechnol. *26*, 117–121.

Liu, H., Styles, C.A., and Fink, G.R. (1996). *Saccharomyces cerevisiae* S288C has a mutation in *FLO8*, a gene required for filamentous growth. Genetics *144*, 967–978.

Lloyd, D., Morrell, S., Carlsen, H.N., Degn, H., James, P.E., and Rowlands, C.C. (1993). Effects of growth with ethanol on fermentation and membrane fluidity of *Saccharomyces cerevisiae*. Yeast *9*, 825–833.

Lorenz, M.C., Cutler, N.S., and Heitman, J. (2000). Characterization of alcohol-induced filamentous growth in *Saccharomyces cerevisiae*. Mol. Biol. Cell *11*, 183–199.

Ma, M., and Liu, L.Z. (2010). Quantitative transcription dynamic analysis reveals candidate genes and key regulators for ethanol tolerance in *Saccharomyces cerevisiae*. BMC Microbiol. *10*, 169.

Madeira, A., Leitão, L., Soveral, G., Dias, P., Prista, C., Moura, T., and Loureiro-Dias, M.C. (2010). Effect of ethanol on fluxes of water and protons across the plasma membrane of *Saccharomyces cerevisiae*. FEMS Yeast Res. *10*, 252–258.

Magasanik, B., and Kaiser, C.A. (2002). Nitrogen regulation in *Saccharomyces cerevisiae*. Gene *290*, 1–18.

Matsuda, F., Ishii, J., Kondo, T., Ida, K., Tezuka, H., and Kondo, A. (2013). Increased isobutanol production in *Saccharomyces cerevisiae* by eliminating competing pathways and resolving cofactor imbalance. Microb. Cell Fact. *12*, 119.

Matsufuji, Y., Fujimura, S., Ito, T., Nishizawa, M., Miyaji, T., Nakagawa, J., Ohyama, T., Tomizuka, N., and Nakagawa, T. (2008). Acetaldehyde tolerance in *Saccharomyces cerevisiae* involves the pentose phosphate pathway and oleic acid biosynthesis. Yeast *25*, 825–833.

Mishra, P., and Prasad, R. (1989). Relationship between ethanol tolerance and fatty acyl composition of *Saccharomyces cerevisiae*. Appl. Microbiol. Biotechnol. *30*, 294–298.

Mitchell, A.P., and Magasanik, B. (1984). Regulation of glutamine-repressible gene products by the *GLN3* function in *Saccharomyces cerevisiae*. Mol. Cell. Biol. *4*, 2758–2766.

Mukhopadhyay, A. (2015). Tolerance engineering in bacteria for the production of advanced biofuels and chemicals. Trends Microbiol. *23*, 498–508.

Mülleder, M., Calvani, E., Alam, M.T., Wang, R.K., Eckerstorfer, F., Zelezniak, A., and Ralser, M. (2016). Functional metabolomics describes the yeast biosynthetic regulome. Cell *167*, 553–565.

Park, S., Chung, S.H., Lu, T., and Sarathy, S.M. (2015). Combustion characteristics of C5 alcohols and a skeletal mechanism for homogeneous charge compression ignition combustion simulation. Energy Fuels *29*, 7584–7594.

Park, S.H., Kim, S., and Hahn, J.S. (2014). Metabolic engineering of *Saccharomyces cerevisiae* for the production of isobutanol and 3-methyl-1-butanol. Appl. Microbiol. Biotechnol. *98*, 9139–9147.

Park, S.H., Kim, S., and Hahn, J.S. (2016). Improvement of isobutanol production in *Saccharomyces cerevisiae* by increasing mitochondrial import of pyruvate through mitochondrial pyruvate carrier. Appl. Microbiol. Biotechnol. *100*, 7591–7598.

Qiu, Z., and Jiang, R. (2017). Improving *Saccharomyces cerevisiae* ethanol production and tolerance via RNA polymerase II subunit Rpb7. Biotechnol. Biofuels *10*, 125.

Robinson, J.S., Klionsky, D.J., Banta, L.M., and Emr, S.D. (1988). Protein sorting in *Saccharomyces cerevisiae*: isolation of mutants defective in the delivery and processing of multiple vacuolar hydrolases. Mol. Cell. Biol. *8*, 4936–4948.

Rødkaer, S.V., and Faergeman, N.J. (2014). Glucose- and nitrogen sensing and regulatory mechanisms in *Saccharomyces cerevisiae*. FEMS Yeast Res. *14*, 683–696.

Scherens, B., Feller, A., Vierendeels, F., Messenguy, F., and Dubois, E. (2006). Identification of direct and indirect targets of the Gln3 and Gat1 activators by transcriptional profiling in response to nitrogen availability in the short and long term. FEMS Yeast Res. *6*, 777–791.

Shively, C.A., Eckwahl, M.J., Dobry, C.J., Mellacheruvu, D., Nesvizhskii, A., and Kumar, A. (2013). Genetic networks inducing invasive growth in *Saccharomyces cerevisiae* identified through systematic genome-wide overexpression. Genetics *193*, 1297–1310.

Sosa, E., Aranda, C., Riego, L., Valenzuela, L., DeLuna, A., Cantú, J.M., and González, A. (2003). Gcn4 negatively regulates expression of genes subjected to nitrogen catabolite repression. Biochem. Biophys. Res. Commun. *310*, 1175–1180.

Stanley, D., Bandara, A., Fraser, S., Chambers, P.J., and Stanley, G.A. (2010). The ethanol stress response and ethanol tolerance of *Saccharomyces cerevisiae*. J. Appl. Microbiol. *109*, 13–24.

Tan, S.Z., Manchester, S., and Prather, K.L. (2016). Controlling central carbon metabolism for improved pathway yields in *Saccharomyces cerevisiae*. ACS Synth. Biol. *5*, 116–124.

Tate, J.J., Buford, D., Rai, R., and Cooper, T.G. (2017). General amino acid control and 14-3-3 proteins Bmh1/2 are required for nitrogen catabolite repression-sensitive regulation of Gln3 and Gat1 localization. Genetics *205*, 633–655.

Trapnell, C., Hendrickson, D.G., Sauvageau, M., Goff, L., Rinn, J.L., and Pachter, L. (2013). Differential analysis of gene regulation at transcript resolution with RNA-seq. Nat. Biotechnol. *31*, 46–53.

Trapnell, C., Pachter, L., and Salzberg, S.L. (2009). TopHat: discovering splice junctions with RNA-Seq. Bioinformatics *25*, 1105–1111.

Trapnell, C., Williams, B.A., Pertea, G., Mortazavi, A., Kwan, G., van Baren, M.J., Salzberg, S.L., Wold, B.J., and Pachter, L. (2010). Transcript assembly and quantification by RNA-Seq reveals unannotated transcripts and isoform switching during cell differentiation. Nat. Biotechnol. *28*, 511–515.

Wach, A., Brachat, A., Pöhlmann, R., and Philippsen, P. (1994). New heterologous modules for classical or PCR-based gene disruptions in *Saccharomyces cerevisiae*. Yeast *10*, 1793–1808.

Winzeler, E.A., Shoemaker, D.D., Astromoff, A., Liang, H., Anderson, K., Andre, B., Bangham, R., Benito, R., Boeke, J.D., Bussey, H., et al. (1999). Functional characterization of the *S. cerevisiae* genome by gene deletion and parallel analysis. Science *285*, 901–906.

Yoshikawa, K., Tanaka, T., Furusawa, C., Nagahisa, K., Hirasawa, T., and Shimizu, H. (2009). Comprehensive phenotypic analysis for identification of genes affecting growth under ethanol stress in *Saccharomyces cerevisiae*. FEMS Yeast Res. *9*, 32–44.

Zhao, E.M., Zhang, Y., Mehl, J., Park, H., Lalwani, M.A., Toettcher, J.E., and Avalos, J.L. (2018). Optogenetic regulation of engineered cellular metabolism for microbial chemical production. Nature *555*, 683–687.

STAR★METHODS

KEY RESOURCES TABLE

REAGENT or RESOURCE	SOURCE	IDENTIFIER
Chemicals, Peptides, and Recombinant Proteins		
SC-Ura medium supplement	Sigma-Aldrich	Cat#Y1501
Yeast extract	BD Biosciences	Cat#212750
Yeast nitrogen base w/o amino acids	BD Biosciences	Cat#291940
Peptone	BD Biosciences	Cat#211677
Casamino acids	BD Biosciences	Cat#223050
Adenine	Nacalai Tesque	Cat#01990-52
L-Glutamic acid	Sigma-Aldrich	Cat#G1501
L-Glutamine	Nacalai Tesque	Cat#16919-42
L-Histidine	Nacalai Tesque	Cat#18119-62
L-Leucine	Nacalai Tesque	Cat#20327-62
Uracil	Nacalai Tesque	Cat#35824-82
L-Glutamic acid-$^{13}C^{5},^{15}N$	Sigma-Aldrich	Cat#607851
L-Glutamine-$^{13}C^{5},^{15}N^{2}$	Taiyo Nippon Sanso	Cat#B06-0008
Agar powder	Nacalai Tesque	Cat#01028-85
Glucose	Nacalai Tesque	Cat#16805-35
G418	Nacalai Tesque	Cat#16513-26
Nourseothricin	Werner BioAgents	Cat#5.001.000
Methanol	Nacalai Tesque	Cat#21915-35
Ethanol	Nacalai Tesque	Cat#14713-95
1-Propanol	Nacalai Tesque	Cat#29109-65
1-Butanol	Wako Pure Chemical Industries	Cat#026-03326
2-Butanol	Wako Pure Chemical Industries	Cat#026-11212
Isobutanol	Nacalai Tesque	Cat#06021-05
tert-Butanol	Sigma-Aldrich	Cat#471712
1-Pentanol	Wako Pure Chemical Industries	Cat#019-03653
2-Methyl-1-butanol	Wako Pure Chemical Industries	Cat#139-08382
Isopentanol	Wako Pure Chemical Industries	Cat#135-12015
1-Hexanol	Wako Pure Chemical Industries	Cat#087-00513
Critical Commercial Assays		
ISOGEN-LS	Nippon Gene	Cat#311-02621
Agilent RNA 6000 Nano Kit	Agilent Technologies	Cat#5067-1511
Agilent High Sensitivity DNA Kit	Agilent Technologies	Cat#5067-4626
KAPA RNA HyperPrep Kit Illumina Platforms	KAPA Biosystems	Cat#KK8540
Deposited Data		
Tolerance factors for strains from yeast deletion library	This study	Table S2
S. cerevisiae (strain S288C) reference genome, version R64-1-1	*Saccharomyces* Genome Database (SGD)	https://downloads.yeastgenome.org/sequence/S288C_reference/genome_releases
Raw and processed RNA-seq data	This study	http://www.ebi.ac.uk/arrayexpress; ArrayExpress: E-MTAB-8175; Table S6
Experimental Models: Organisms/Strains		
S. cerevisiae: BY4741 (S288C *MAT***a** *his3Δ1 leu2Δ0 met15Δ0 ura3Δ0*)	Euroscarf	Y00000
S. cerevisiae: BY4743 (S288C *MAT***a**/α *his3Δ1/his3Δ1 leu2Δ0/leu2Δ0 LYS2/lys2Δ0 met15Δ0/MET15 ura3Δ0/ura3Δ0*)	Euroscarf	Y20000

(*Continued on next page*)

Continued

REAGENT or RESOURCE	SOURCE	IDENTIFIER
S. cerevisiae: CEN.PK2-1C (*MAT***a** *his3Δ1 leu2-3,112 ura3-52 trp1-289 MAL2-8c SUC2*)	Euroscarf	30000A
S. cerevisiae: SEY6210 (*MATα leu2-3,112 ura3-52 his3-Δ200 trp1-Δ901 suc2-Δ9 lys2-801 Gal*)	ATCC	96099
S. cerevisiae: BY4741-derivative deletion strains	Euroscarf	Table S9
S. cerevisiae: Strains constructed in this study	This study	Table S9
Oligonucleotides		
Primers used in this study	This study	Table S11
Recombinant DNA		
Plasmids for overexpressing PPP genes by 2μm *URA3* plasmid containing the endogenous promoter, ORF, and terminator sequence	Huang et al., 2013	Table S10
Plasmid: pRS426 (empty plasmid with 2μm and *URA3*)	Christianson et al., 1992	ATCC: 77107
Plasmid: pJA184 (2μm *URA3* plasmid for isobutanol production)	Avalos et al., 2013	Table S10
Plasmid: pYZ84 (*lox66-natMX6-lox71* deletion cassette)	Hammer and Avalos, 2017	Table S10
Plasmid: pUG6 (*loxP-kanMX4-loxP* deletion cassette)	Gueldener et al., 2002	Table S10
Software and Algorithms		
GO Term Finder	Boyle et al., 2004	https://www.yeastgenome.org/goTermFinder
TopHat (Version 2.0.9)	Trapnell et al., 2009	http://ccb.jhu.edu/software/tophat/index.shtml
PicardTools (Version 1.105)	Broad Institute	http://broadinstitute.github.io/picard
Cufflinks (Version 2.2.1)	Trapnell et al., 2010	https://github.com/cole-trapnell-lab/cufflinks
Cuffdiff (Version 2.2.1)	Trapnell et al., 2013	http://cole-trapnell-lab.github.io/cufflinks/cuffdiff/

LEAD CONTACT AND MATERIALS AVAILABILITY

Further information and requests for resources and reagents should be directed to and will be fulfilled by the Lead Contact, José L. Avalos (javalos@princeton.edu).

Materials Availability Statement

All strains and plasmids generated in this study are available from the Lead Contact with a completed Materials Transfer Agreement.

EXPERIMENTAL MODEL AND SUBJECT DETAILS

Yeast Strains and Media

The *Saccharomyces cerevisiae* strains (BY4741, BY4743, CEN.PK2-1C, SEY6210) (Brachmann et al., 1998; Entian and Kötter, 2007; Robinson et al., 1988) and their derivatives used in this study are listed in Table S9. For all screens and analyses of alcohol tolerance, wild type and deletion strains were cultured in synthetic complete (SC) medium made inhouse (Table S8) at 30°C, and 2% glucose. Strains overexpressing PPP genes were cultured in SC medium lacking uracil (SC-Ura) made inhouse. For isobutanol production experiments, strains were fermented in 0.67% (w/v) yeast nitrogen base without amino acids, 0.192% (w/v) of a commercially available SC-Ura medium supplement (Sigma-Aldrich, Y1501) (Figure 6; Table S8), as well as media made inhouse (Figure S10; Table S8), both containing 15% (w/v) glucose. Transformants complemented with *TRP1* were selected on agar plates with minimal synthetic defined (SD) medium [0.67% (w/v) yeast nitrogen base without amino acids, 2% (w/v) glucose, 0.5% (w/v) casamino acids, 0.002% (w/v) adenine, 0.002% (w/v) L-histidine, 0.012% (w/v) L-leucine, and 0.002% (w/v) uracil]. Transformants with open reading frame (ORF) deletions generated by insertion of the *kanMX4* or *natMX6* markers were selected on YPD [1% (w/v) yeast extract, 2% (w/v) Bacto peptone, and 2% (w/v) glucose] agar plates containing 200 μg/mL G418 (Nacalai Tesque) or 200 μg/mL nourseothricin (Werner BioAgents, Jena, Germany), respectively. Transformants harboring 2μ plasmids to overexpress a single PPP gene under the control of its native promoter (Table S10) were selected on SC-Ura agar plates. All yeast transformations were performed using a standard lithium acetate method (Ito et al., 1983).

METHOD DETAILS

Screen of the Yeast Knockout Collection

Deletion mutants showing increased sensitivity or tolerance to isobutanol were isolated from the deletion collection of non-essential genes derived from the haploid BY4741 strain (Euroscarf, Frankfurt, Germany) (Winzeler et al., 1999), as described below. The wild type BY4741 strain and deletion strains were inoculated into 200 μL of SC medium in 96-well microplates (Falcon 353072; Corning, NY, USA) using a 96-pin replicator and pre-cultured at 30°C for 24 hrs without shaking. For the initial screen, 5 μL of each pre-culture was inoculated into 195 μL of SC medium containing isobutanol at a final concentration of 1.4% (v/v) and SC medium without isobutanol. The microplates were sealed with aluminum foil tape (3M, MN, USA) to minimize evaporation and prevent contamination, and then incubated at 30°C for 24 hrs without shaking. After removing the tape, the optical density at 600 nm (OD_{600}) of each well was measured with a Tecan Safire 2 microplate reader (Tecan). A tolerance factor was calculated using the following formula: tolerance factor = (OD_{600} with isobutanol) / (OD_{600} without isobutanol) (Table S2). During the screens, the wild type BY4741 strain showed a tolerance factor of 0.38 in the presence of 1.4% (v/v) isobutanol (Tables S1 and S2). Deletion strains with tolerance factors < 0.2 (1025 strains) or > 0.8 (517 strains) in 1.4% isobutanol were defined as isobutanol-sensitive or -tolerant, respectively, and underwent the second screen. Mutants exhibiting poor growth without isobutanol (OD_{600} < 0.5) were excluded from subsequent screens. To isolate the most sensitive deletion strains, the second screen utilized reduced isobutanol concentrations of 1.2% and 0.6%. The second screen was repeated for the 164 most sensitive strains identified under these conditions to confirm the sensitive phenotypes of these deletion strains (n = 3). After the second screen, the 46 deletion strains with tolerance factors < 0.5 in 0.6% isobutanol or tolerance factors < 0.1 in 1.2% isobutanol were defined as hypersensitive.

To identify deletion strains hypertolerant to isobutanol, a second set of screens in media containing 1.5% or 1.6% (v/v) isobutanol was performed. During these screens, the tolerance factor of the wild type BY4741 strain in the presence of 1.5% or 1.6% isobutanol was 0.19 or 0.11, respectively (Table S1). The second screen was repeated for the 36 most tolerant strains identified under these conditions to confirm the tolerant phenotypes of these deletion strains (n = 3). After the second screen, the 6 deletion mutants exhibiting tolerance factors > 0.4 in 1.5% isobutanol were defined as isobutanol hypertolerant.

Analysis of Data from Deletion Mutant Screens

Tolerance factor data from the second screen of the 164 most sensitive and the 36 most tolerant strains were sorted in descending order based on those in 0.6% and 1.5% (v/v) isobutanol, respectively. Heat maps from the sorted tolerance factor data were generated using Microsoft Excel (Figures 1B and 1C). The data of wild-type strain was attached to the left end of the heat maps. GO term enrichment analysis was performed using the GO Term Finder (https://www.yeastgenome.org/goTermFinder) (Boyle et al., 2004).

Construction of Complementation, Deletion, and Overexpression Strains

All primers used for strain construction are listed in Table S11. For complementation of the *trp1* auxotrophy in laboratory strains CEN.PK2-1C and SEY6210, a *TRP1* DNA fragment containing its promoter, ORF, and terminator amplified from BY4741 genomic DNA by PCR using the primers TRP1-Pro-F and TRP1-Term-R was used to transform CEN.PK2-1C and SEY6210 wild type strains. Transformants carrying a functional *TRP1* gene (CEN. PK2-1C *TRP1* and SEY6210 *TRP1*) were selected on SD agar plates.

Deletion strains reconstructed in BY4741 and CEN.PK2-1C *TRP1* were generated using a PCR-based gene disruption method (Wach et al., 1994). Each of the target ORFs (*GND1*, *ZWF1*, and *GLN3*) was replaced by the *kanMX4* gene. This was achieved by PCR amplifying DNA fragments consisting of the 5′ flanking sequence of the ORF, the *kanMX4* gene, and the 3′ flanking sequence of the ORF from the genomic DNA of the corresponding BY4741 deletion strain (Euroscarf). BY4741 and CEN.PK2-1C *TRP1* strains were transformed with the amplified DNA fragments and selected on YPD plates with the corresponding selective antibiotic. The gene deletions were confirmed by PCR with forward primers annealing upstream of the introduced DNA fragment and reverse primers annealing within the antibiotic resistance marker. Gene deletions in BY4741 isobutanol production strains were constructed and verified in a similar manner, except *lox* sites were added to the deletion cassettes, such that antibiotic resistance markers could be recovered if needed. Thus, *lox66-natMX6-lox71* cassette in pYZ84 (Hammer and Avalos, 2017) and *loxP-kanMX4-loxP* cassette in pUG6 (Gueldener et al., 2002) were PCR-amplified with 5′ and 3′ homology to *GLN3* and *ALD6*, respectively (Tables S10 and S11). To overexpress PPP genes, 2μ plasmids harboring *GND1*, *GND2*, *ZWF1*, *TKL1*, *TKL2*, *TAL1*, *SOL3*, or *RPE1*, each under the control of their native promoters and terminators (Huang et al., 2013) (Table S10), were introduced into the wild type BY4741 strain.

Analysis of Alcohol Tolerance after Screening

The tolerance of yeast strains to each of the alcohols tested was analyzed in liquid culture in 96-well microplates; tolerance to isobutanol and ethanol was also analyzed on agar plates. Yeast cells were pre-cultured in liquid SC or SC-Ura medium at 30°C for 24 hrs. For experiments performed in liquid medium, each pre-culture was diluted with sterilized water to an OD_{600} of 4. Five microliters of diluted pre-culture were inoculated into 195 μL of SC or SC-Ura medium containing various concentrations of alcohols, near their corresponding LC_{50} concentrations for the wild type BY4741, to obtain a starting OD_{600} of 0.1. The 96-well microplates were sealed with aluminum foil tape (3M), and incubated at 30°C for 24 hrs. After removing the tape, OD_{600} value of each well was measured with a Tecan Safire 2 or VMax (Molecular Devices, CA, USA) microplate reader.

For analysis on agar plates, pre-cultures were diluted with sterilized water to an OD_{600} of 0.2, and 10 μL samples were spotted onto SC or SC-Ura agar plates supplemented with various concentrations of isobutanol (1.0%, 1.5%, 1.8%, 2.1%, 2.4%, 2.7%, or 3.0%) or ethanol (8% or 10%), with each subsequent spot diluted 2-fold. The agar plates were sealed with vinyl tape and incubated at 30°C for 2 to 4 d.

RNA-Seq Analysis

Wild-type BY4741 and BY4741 *gln3Δ* strains were pre-cultivated in liquid SC medium made inhouse at 30°C for 24 hrs. Each pre-culture was inoculated into fresh liquid SC medium made inhouse with or without 1.3% (v/v) isobutanol to obtain a starting OD_{600} of 0.1. Cultivation was performed in test tubes with screw caps at 30°C for 12 hrs with 240 rpm shaking. Cells were harvested at 3,000 × *g* for 5 min at room temperature. Total RNA was extracted from each culture with Isogen-LS (Nippon Gene, Tokyo, Japan), as described previously (Chomczynski and Sacchi, 2006). RNA integrity was evaluated for quality control with an Agilent Bioanalyzer 2,100 using Agilent RNA 6,000 Nano Kit (Agilent Technologies, CA, USA). Preparation of cDNA libraries was performed using KAPA RNA HyperPrep Kit Illumina Platforms (Kapa Biosystems, MA, USA). Prepared cDNA libraries were validated with an Agilent Bioanalyzer 2,100 using an Agilent High Sensitivity DNA Kit (Agilent Technologies), and sequenced on Illumina MiSeq (75-bp nucleotide paired-end sequence).

The RNA-seq reads were mapped to the *S. cerevisiae* S288c genome sequence (version R64-1-1, *Saccharomyces* Genome Database) using TopHat (version 2.0.9) (Trapnell et al., 2009). PicardTools (version 1.105, https://broadinstitute.github.io/picard/) were used to sort the mapped reads and remove PCR duplicates. Transcript quantification, reported as FPKM (fragments per kilobase of transcript per million fragments mapped) from RNA-seq data, was performed by Cufflinks (version 2.2.1) (Trapnell et al., 2010). To improve the robustness of the estimation of differential expression, the reads mapping to rRNA, tRNA, and non-coding RNA were excluded from the quantification. Cuffdiff (version 2.2.1) (Trapnell et al., 2013) was used to normalize the data sets and calculate the fold changes and their statistical significance of two independent biological replicates. To avoid infinite fold changes, a value of one was added to all the FPKM values. The adjusted FPKM values were log2-transformed, and row Z-scores for each gene were calculated relative to the $\log_2$ FPKM of each gene in the wild type strain grown without isobutanol. Heat maps from hierarchically clustered Z-scores by Cluster3.0 (Eisen et al., 1998) were generated using Microsoft Excel. Volcano plots were generated using the R software and the package EnhancedVolcano (https://github.com/kevinblighe) from Bioconductor.

Quantification of Intracellular Amino Acids

Wild-type BY4741 and BY4741 *gln3Δ* strains were cultivated and collected as for the RNA-seq analysis. After washing the 3.2×10^7 cells with distilled water twice, metabolites were extracted as described previously (Mülleder et al., 2016). For metabolite extraction, cells were incubated with 200 μL of hot 98.5% ethanol (80°C) containing isotopically labeled amino acid standards, L-glutamic acid-$^{13}C_5$,^{15}N (Sigma-Aldrich, 607851) and L-glutamine-$^{13}C_5$,$^{15}N_2$ (Taiyo Nippon Sanso, Tokyo, Japan, B06-0008) at 80°C for 2 min. The standards were used for normalizing quantification data of each amino acid among the extracts. After vigorous mixing by a vortex mixer, the extracts were incubated at 80°C for another 2 min. Cell debris were removed by centrifugation at 10,000 × *g* for 1 min. The resulting extracted metabolites and culture supernatants were subjected to LC-MS/MS analysis.

Amino acids were separated by a reversed-phase/cation-exchange/anion-exchange tri-modal column (Scherzo SS-C18 column, 100 mm × 3 mm, 3 μm, Imtakt, Kyoto, Japan) on a high performance liquid chromatography instrument (Nexera system; Shimadzu, Kyoto, Japan) and triple quadrupole mass spectrometer (LCMS-8060; Shimadzu). A gradient elution was performed by changing the mixing ratio of eluent A, composed of 0.1% (v/v) formic acid in water, and eluent B, composed of 60 mM ammonium sulfate and 40% (v/v) acetonitrile in water. The gradient began with an isocratic elution of 5% B for 3 min, followed by linear gradient elution from 5% to 100% B over 5 min. Then, the solvent composition was held at 100% B for 3 min, and immediately returned to 5% B over 2 min. The flow rate was 0.3 mL/min for the first 3 min and 0.6 mL/min for the next 10 min. The column temperature was maintained at 40°C throughout the analysis. Glutamic acid and glutamine were quantified in multiple reaction monitoring (MRM) mode using triple quadrupole mass spectrometry (LCMS-8060) with an electrospray ionization source (ESI). Parameters including *m/z* transition and retention time are listed in Table S12. To calculate the intracellular concentrations of amino acids from the data of MRM analysis, the values for 3.2×10^7 cells/mL per OD_{595} and cell volume (45.54 fL) for the BY4741 strain were used.

Measurement of Intracellular NADPH/$NADP^+$ Ratios

Wild-type BY4741 and BY4741 *gln3Δ, gnd1Δ*, and *zwf1Δ* strains were cultivated in liquid SC medium made inhouse with or without 0.4% (v/v) isobutanol (for *gnd1Δ* and *zwf1Δ* strains) or 1.3% isobutanol (for *gln3Δ* strain). A lower concentration of isobutanol was used for *gnd1Δ* and *zwf1Δ* strains due to their high isobutanol sensitivity (Figure 2A). Strains grown without isobutanol were cultivated in 10 mL SC medium in 50 mL screw-cap falcon tubes at 30°C for 16 hrs with 200 rpm shaking. Strains grown with isobutanol were cultivated in 20 mL SC medium in 250 mL flasks at 30°C for 20 hrs with 200 rpm shaking. After overnight growth, 1 mL samples of strains grown without isobutanol were centrifuged for 1 min at 13,000 rpm; 10 mL samples of strains grown with isobutanol were centrifuged for 3 min at 3,000 rpm. After supernatant was discarded, intracellular NADPH and $NADPH^+$ were extracted using sodium hydroxide and hydrochloric acid as previously described (Kern et al., 2014). Samples were either frozen at -80°C or analyzed immediately. An enzyme-cycling assay employing phenazine ethosulfate (PES, Sigma-Aldrich P4544) and methylthiazolyldiphenyl-tetrazolium bromide (MTT, Sigma-Aldrich M2128) was used to determine intracellular NADPH and $NADP^+$ concentrations (Kern et al.,

2014), with absorbance at 570 nm monitored using a TECAN Infinite 200 Pro microplate reader. NADPH (Sigma-Aldrich, 10107824001) and $NADP^+$ (Sigma-Aldrich, 10128031001) standards were prepared fresh with each assay measurement.

Microscopy

Yeast cells were observed using an inverted microscope IX71 (Olympus, Tokyo, Japan) equipped with an UPlanSApo 100×/1.40 oil objective (Olympus). Phase contrast images were obtained using Aqua-Cosmos 2.0 software (Hamamatsu Photonics, Shizuoka, Japan) and a digital charge-coupled device camera (C4742-95-12ER, Hamamatsu Photonics).

Construction of Isobutanol-Producing Yeast Strains

After deletion of *ALD6* and/or *GLN3*, the five genes in the biosynthetic pathway from pyruvate to isobutanol were overexpressed in a single 2μ plasmid. The 2μ plasmid introduced, pJA184 (Avalos et al., 2013), contains *ILV2, ILV3, ILV5*, with their gene products targeted to mitochondria; and an α-ketoacid decarboxylase (KDC) from *Lactococcus lactis* (*LlKivD*) and an alcohol dehydrogenase (*ADH7*), with their gene products targeted to the cytosol. Wild type and isobutanol-tolerant strains were transformed with either plasmid pJA184 for expression of the five genes in their natural compartments, or empty plasmid pRS426 (Christianson et al., 1992) as a negative control. Transformants were isolated on SC-Ura agar plates incubated at 30°C for 2 to 4 d. Because a wide range of colony sizes, growth rates, and isobutanol productivity can result from 2μ plasmid transformations, 8 – 12 colonies from each transformation were screened to identify those producing the most isobutanol.

Fermentations for Isobutanol Production

Single colonies from the transformations were cultured in 5 mL of SC-Ura medium in 14 mL round-bottom falcon tubes (Corning, NY, USA) at 30°C for 24 hrs, followed by centrifugation at 2,000 × *g* for 3 min. Cell pellets were re-suspended in 5 mL of SC-Ura medium containing 10% (w/v) glucose and cultured under semi-aerobic conditions at 30°C with 250 rpm agitation for 24 hrs. After measuring the OD_{600} of each culture, cells were recovered by centrifugation for 3 min at 2,000 × *g* and re-suspended in SC-Ura medium containing 15% (w/v) glucose to obtain a starting OD_{600} of 15. After transferring 5 mL of each diluted culture to a new 14 mL round-bottom tube, fermentations were carried out under semi-aerobic conditions at 30°C with 250 rpm agitation for 24 hrs.

Quantitative Determination of Isobutanol Production

Concentrations of isobutanol in the supernatant after 24 hrs fermentations were measured by high-performance liquid chromatography (HPLC). Cell cultures were centrifuged at 12,000 × *g* and 4°C for 2 min, and the supernatant was filtered through Ultrafree-MC centrifugal filter units (0.45 μm; Millipore, MA, USA). Filtered supernatant (200 μL) was analyzed using an HPLC system consisting of a pump (LC-20AD, Shimadzu), autosampler (SIL-20A, Shimadzu), degasser (DGU-14A, Shimadzu), column oven (CTO-20A, Shimadzu), refractive index (RI) detector (RID-10A, Shimadzu), and Aminex HPX-87H column (Bio-Rad, CA, USA). The column was eluted with 5 mM H_2SO_4 at a flow rate of 0.6 mL/min and 55°C. To determine the isobutanol concentration in each sample, peak areas from the chromatographic data, monitored by the RI detector, were compared to those of freshly prepared isobutanol standards using LC Solution software (Shimadzu).

QUANTIFICATION AND STATISTICAL ANALYSIS

Error bars represent the SEM of three, four, or six independent experiments. Statistical significance was evaluated by a two-tailed Student's *t*-test. Statistical details for each experiment can be found in the Figure Legends. GO term enrichment analysis was performed using the GO Term Finder (https://www.yeastgenome.org/goTermFinder) (Boyle et al., 2004).

DATA AND CODE AVAILABILITY

Complete data sets of tolerance factors for strains from yeast deletion library in the initial screen are available in Table S2. Data sets of genes whose deletion leads to sensitivity or confers highest tolerance to isobutanol in the second screen are available in Tables S3 and S4, respectively. Complete RNA-seq data are available in Table S6.The accession number for the RNA-seq data reported in this paper is ArrayExpress: E-MTAB-8175.

Cell Systems, Volume *9*

Supplemental Information

Critical Roles of the Pentose Phosphate Pathway and *GLN3* in Isobutanol-Specific Tolerance in Yeast

Kouichi Kuroda, Sarah K. Hammer, Yukio Watanabe, José Montaño López, Gerald R. Fink, Gregory Stephanopoulos, Mitsuyoshi Ueda, and José L. Avalos

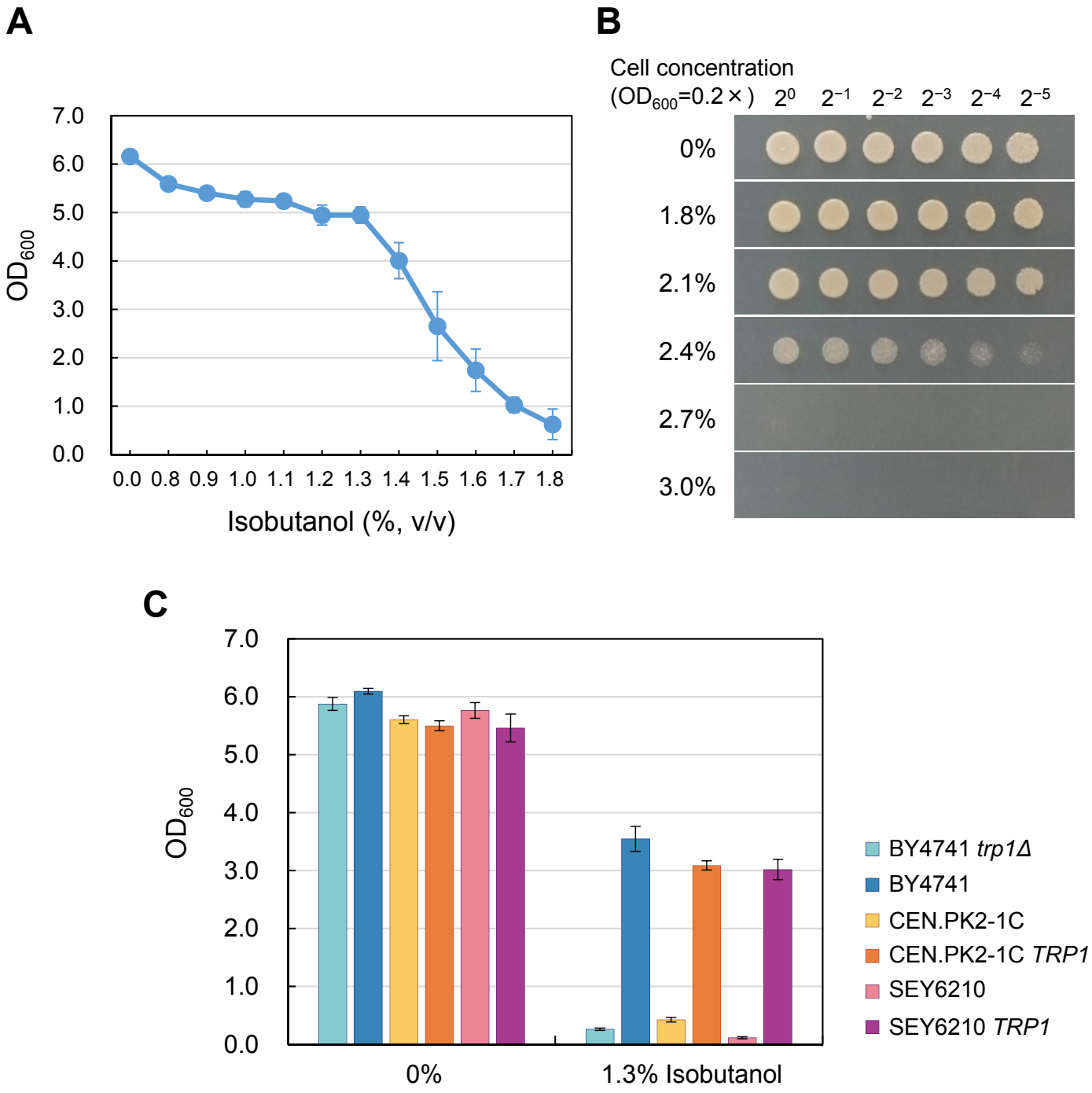

Figure S1. Cell growth of the BY4741 wild-type strain in synthetic complete (SC) liquid medium containing isobutanol and effect of *trp1Δ* allele in wild-type laboratory strains (related to Figure 1). Cell growth of the BY4741 wild-type strain was monitored in SC liquid medium (A) and solid medium (B) after 24 h of cultivation at 30°C. (C) Cell growth of the wild-type strains (BY4741, CEN.PK2-1C, and SEY6210) with or without *TRP1* was measured in liquid SC medium containing 1.3% (v/v) isobutanol. Error bars represent the SEM of three independent experiments.

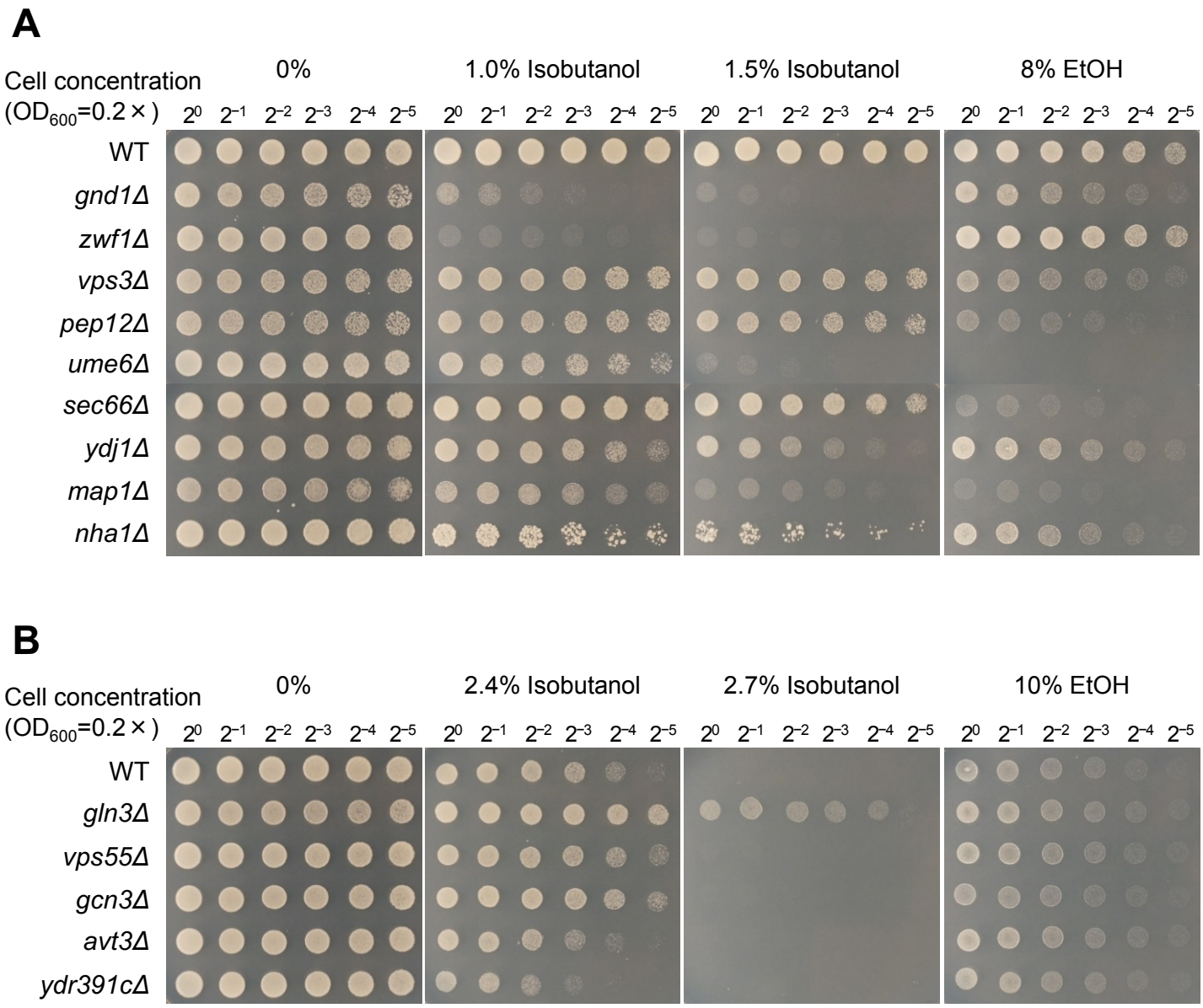

Figure S2. Cell growth of most hypersensitive and hypertolerant strains to isobutanol in solid medium containing isobutanol or ethanol (related to Figures 2 and 4). Cell suspensions (10 µL) of isobutanol-hypersensitive strains in Figure 2A (A) and isobutanol-hypertolerant strains (B) were spotted on SC agar plates. Each subsequent spot represents a 2-fold dilution. Plates were incubated at 30°C for 48 h.

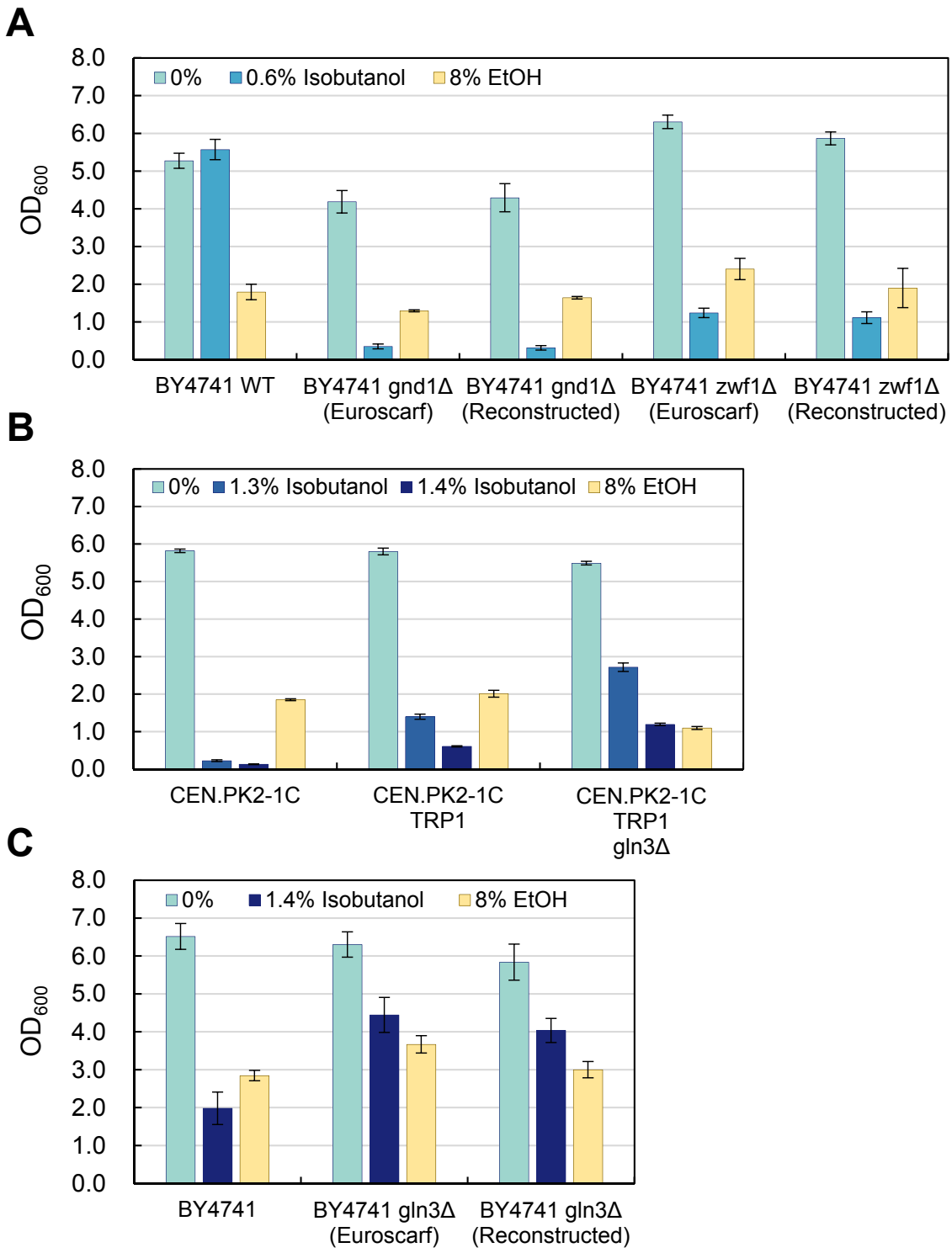

Figure S3. Isobutanol and ethanol sensitivity of reconstructed deletion strains in BY4741 and CEN.PK2-1C background (related to Figures 2 and 4). (A) Cell growth of the reconstructed BY4741 *gnd1Δ* and BY4741 *zwf1Δ* strains was measured in liquid SC medium containing 0.6% (v/v) isobutanol or 8% Ethanol. (B) Cell growth of the *TRP1*-restored CEN.PK2-1C strain and its derivative *gln3Δ* strain was measured in liquid SC medium containing 1.3% isobutanol, 1.4% isobutanol, or 8% Ethanol. (C) Cell growth of the reconstructed BY4741 *gln3Δ* strain was measured in liquid SC medium containing 1.4% isobutanol or 8% Ethanol. Error bars represent the SEM of three independent experiments.

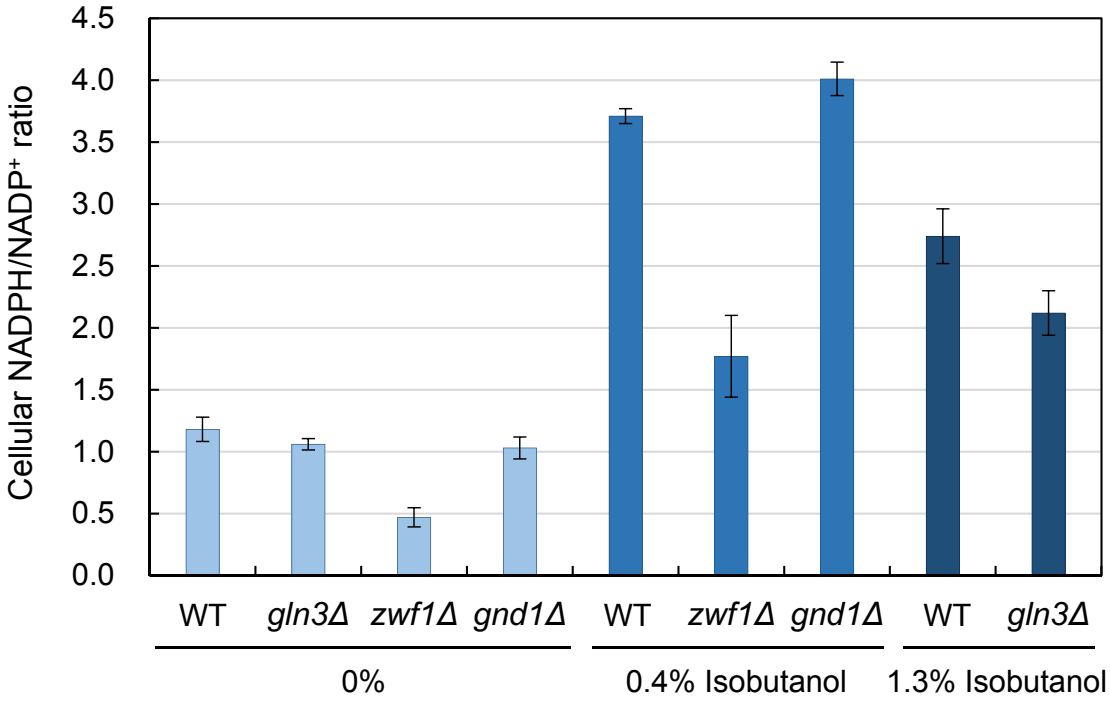

Figure S4. Cellular NADPH/NADP$^+$ ratios of yeast deletion strains (related to Figures 2 and 3). Wild type, *gln3Δ*, *zwf1Δ*, and *gnd1Δ* strains were cultivated in liquid SC medium without isobutanol at 30^{o}C for 16 h and SC medium containing 0.4% (v/v) or 1.3% isobutanol at 30^{o}C for 20 h. Error bars represent the SEM of four (for experiments with 0.4% isobutanol), six (for WT and *zwf1Δ* without isobutanol and experiments with 1.3% isobutanol), and eight (for *gln3Δ* and *gnd1Δ* without isobutanol) independent experiments.

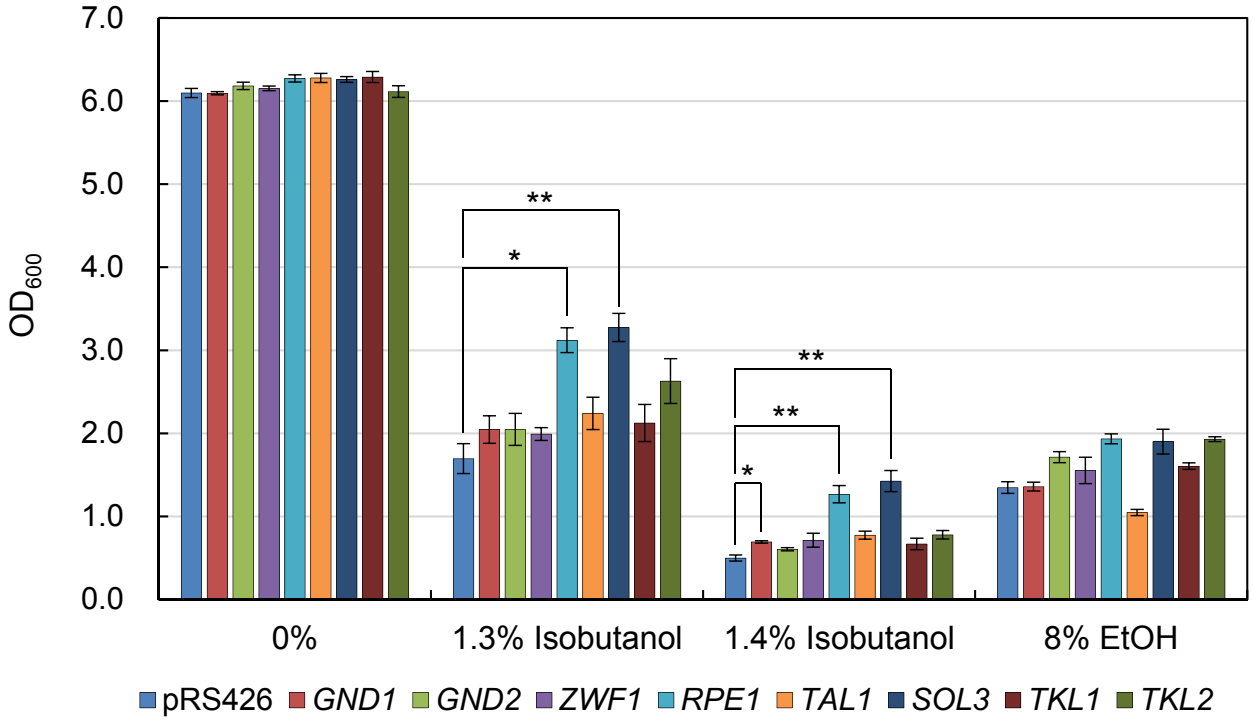

Figure S5. Isobutanol tolerance of BY4741 strains overexpressing 2μ plasmids with single PPP genes (related to Figures 2 and 3). Single PPP genes were expressed under the control of their native promoters and terminators. The strains overexpressing PPP genes were cultivated in liquid SC-ura medium containing 1.3% (v/v) or 1.4% isobutanol, or 8% Ethanol at 30°C for 24 h. Error bars represent the SEM of six independent experiments. A two-tailed student's *t*-test was used to assess the statistical significance of the difference between cell growths of control and PPP gene-overexpressing strains in the presence of isobutanol; *$p < 0.001$, **$p < 0.0001$.

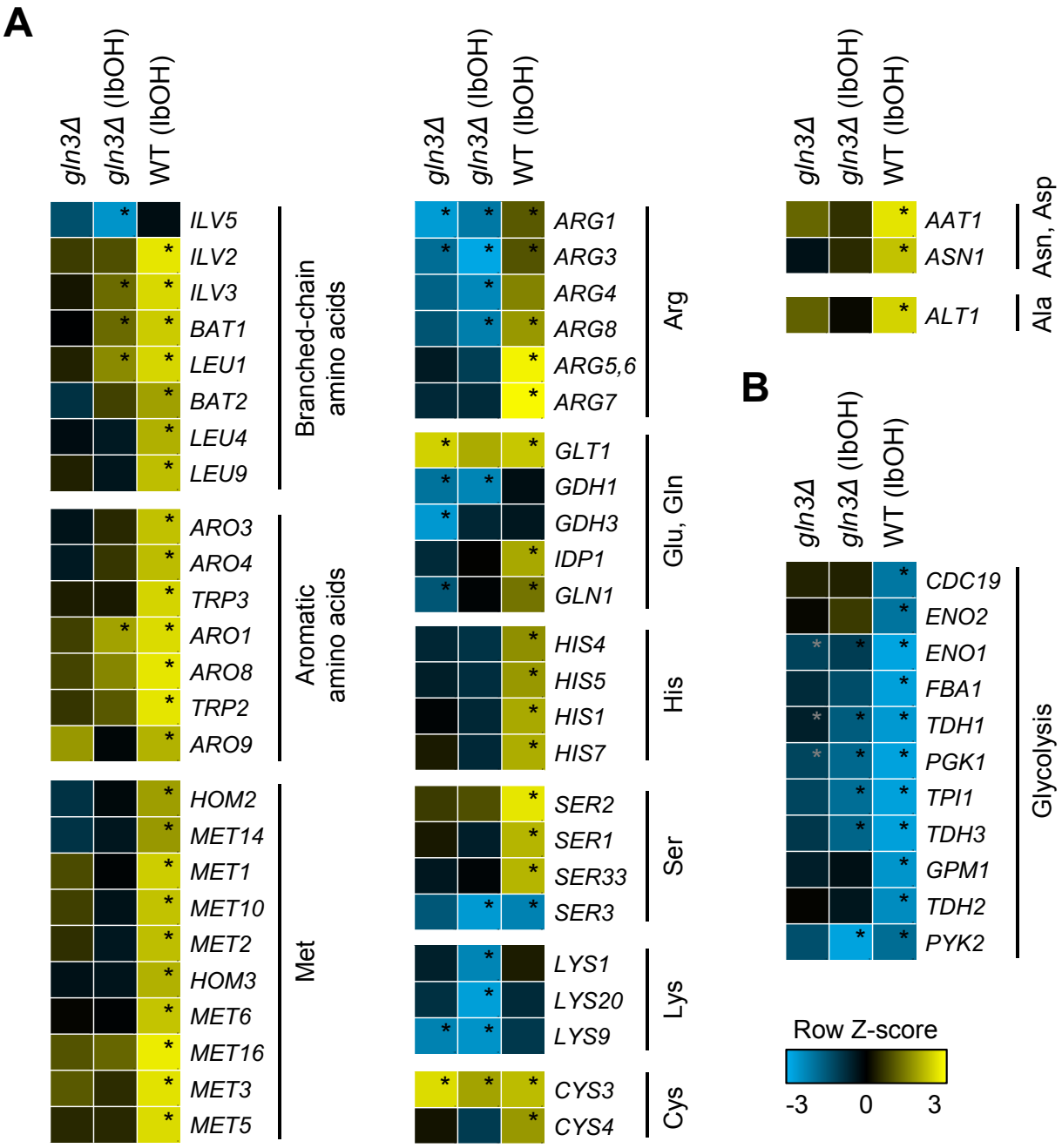

Figure S6. Heat maps showing expression profiles of genes involved in amino acid biosynthesis and glycolysis (related to Figure 4). Expression levels of genes involved in amino acid biosynthesis (A) and glycolysis (B) are shown as row Z-score that is the number of standard deviations away from $\log_2$FPKM of the wild type strain grown without isobutanol. Genes in each category were hierarchically clustered with row Z-scores. The statistical significance of the difference from FPKM in the wild type strain grown without isobutanol is shown; *$p < 0.05$.

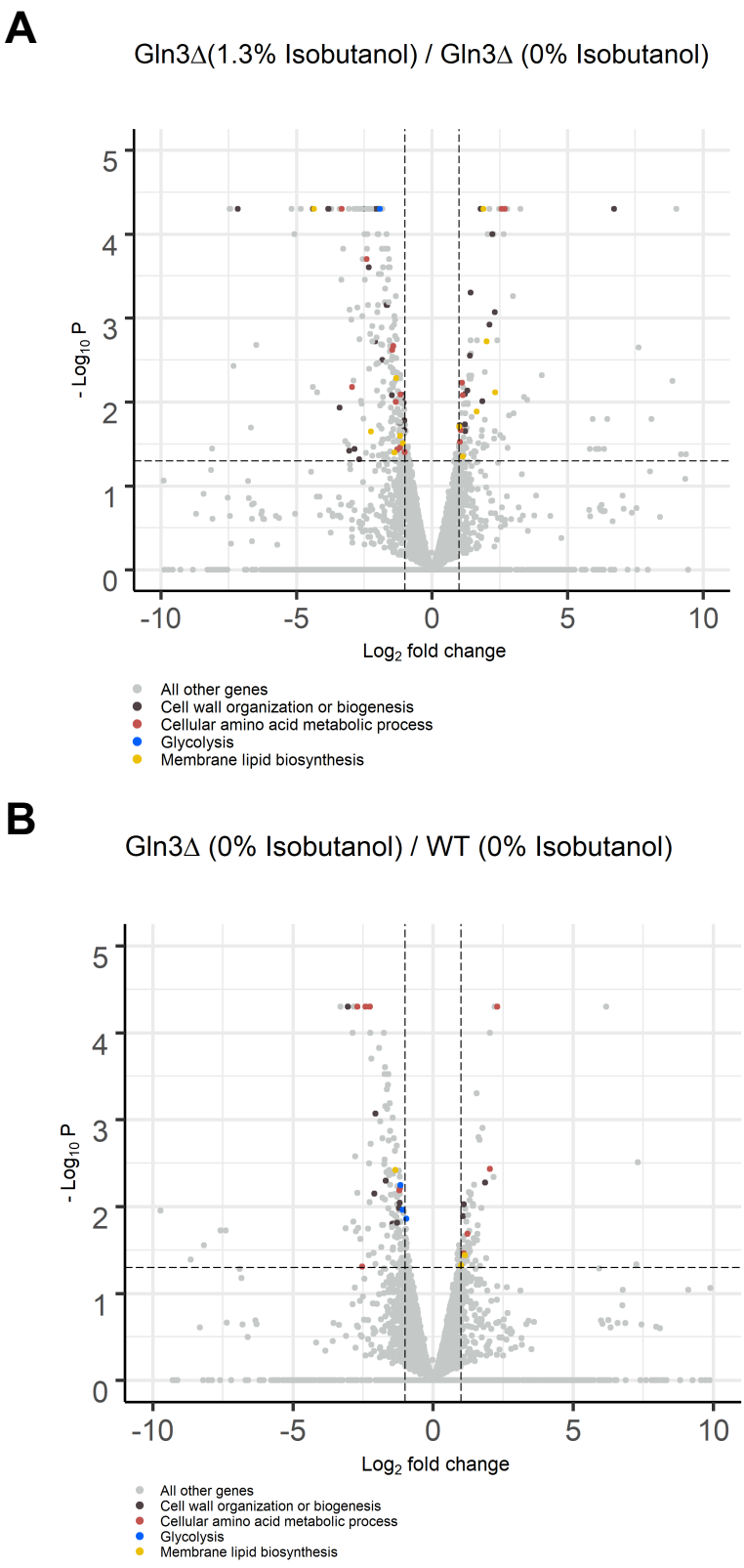

Figure S7. Volcano plots representing differentially expressed genes (related to Figure 5). (A) Comparison of the transcriptomic profiles between the *gln3Δ* strain grown with 1.3% (v/v) isobutanol and the *gln3Δ* strain grown without isobutanol. (B) Comparison of the transcriptomic profiles between the *gln3Δ* strain grown without isobutanol and the wild type strain grown without isobutanol. Each dot represents one gene whose position is determined by the average $\log_2$ fold change and negative $\log_{10}$ *p*-value from two independent experiments. The differentially expressed genes are identified on the basis of $|\text{Log}_2$ fold change$| > 1$ and *p*-value < 0.05. Genes labeled as involved in "glycolysis" are one of the following: *CDC19, ENO1, ENO2, FBA1, GPM1, PGK1, PYK2, TPI1, TDH1, TDH2, TDH3.* Genes labeled as involved in "membrane lipid biosynthesis" are one of the following: *ACP1, ARE1, AYR1, CHO1, DPP1, EEB1, ELO1, ERG3, ERG4, FAS1, GPC1, HES1, HFD1, HMG2, ICT1, INO1, INP54, LAC1, LSB6, MCR1, OLE1, OPI3, ORM2, PDR16, PLB2, SCS2, SEC59, TAM41, TCB3, TGL2, TSC10, YDC1, YDR018C, YEH1.*

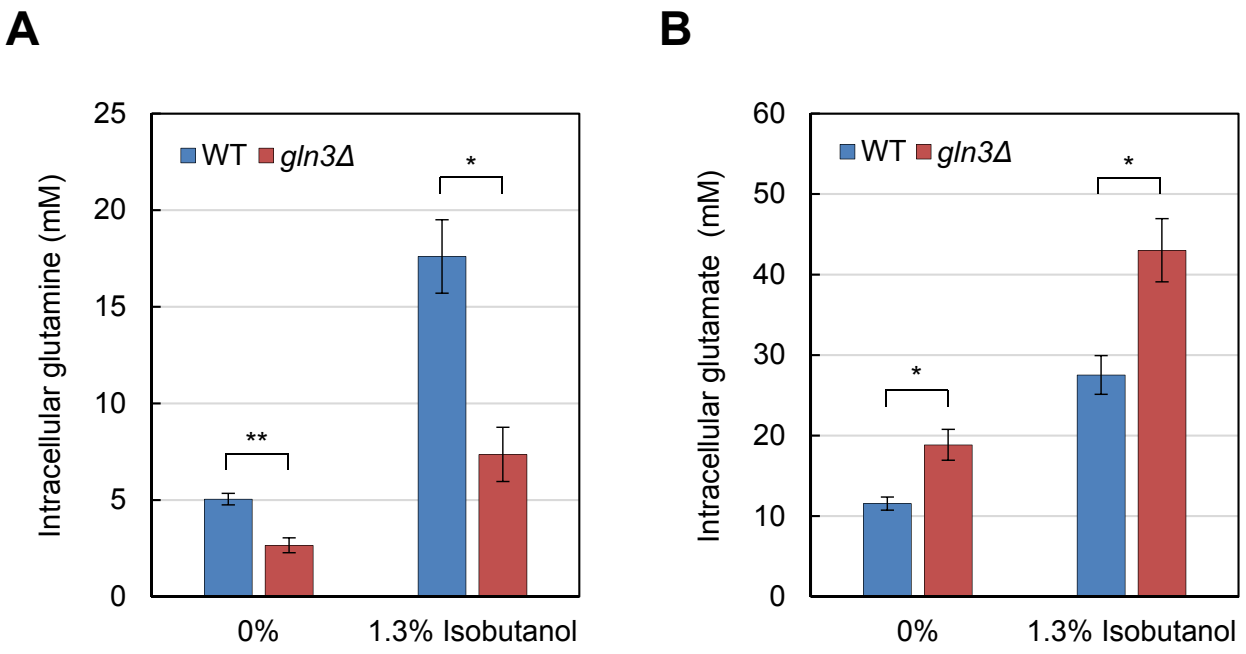

Figure S8. Intracellular concentrations of glutamine and glutamate in different conditions (related to Figure 4). Wild type and *gln3Δ* strains were grown in SC medium with or without 1.3% (v/v) isobutanol at 30°C for 12 h. The concentrations of glutamine (A) and glutamate (B) in the metabolites extracted from cells were measured by multiple reaction monitoring (MRM) mode using LC-MS/MS. A two-tailed student's *t*-test was used to assess the statistical significance of the difference between the amino acid concentrations in wild type and *gln3Δ* strains; $*p < 0.01$, $**p < 0.001$. Error bars represent the SEM of six independent experiments.

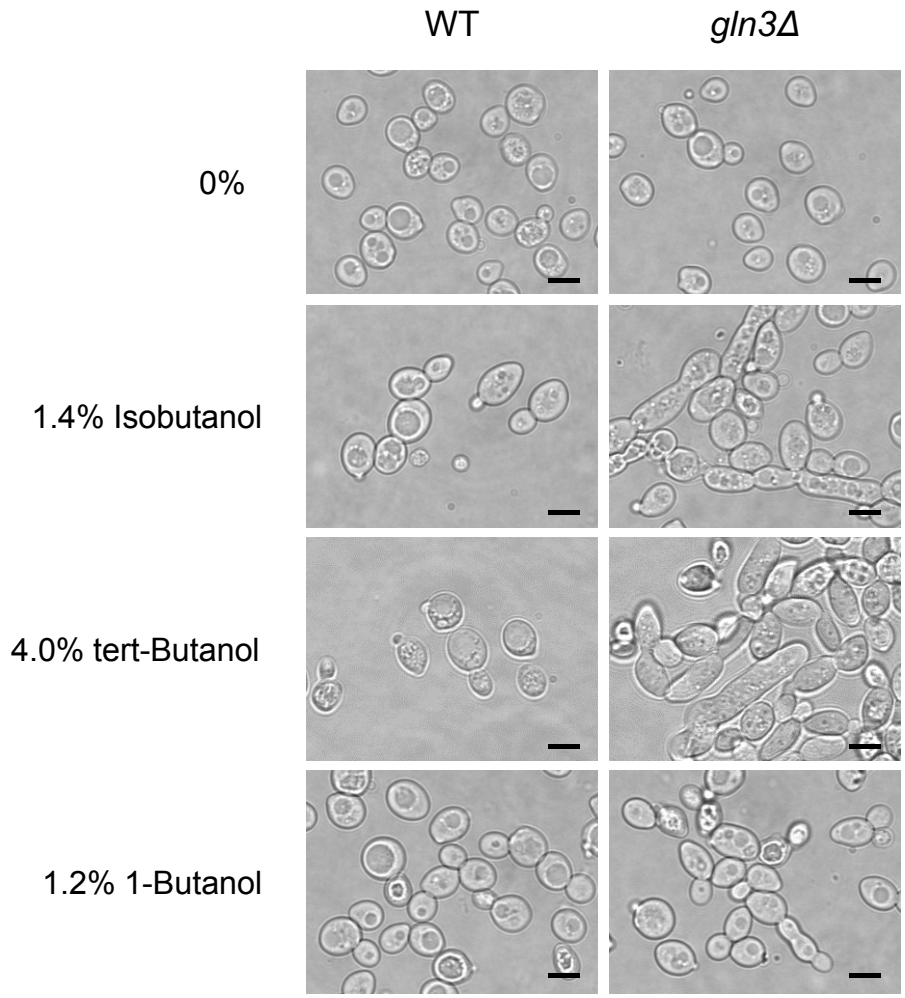

Figure S9. Morphologies of yeast deletion strains grown with alcohols (related to Figures 2 and 4). Wild type and *gln3Δ* strains were cultivated in liquid SC medium containing 1.4% (v/v) isobutanol, 4.0% tert-butanol, or 1.2% 1-butanol at 30°C for 24 h. Scale bars indicate 5 μm.

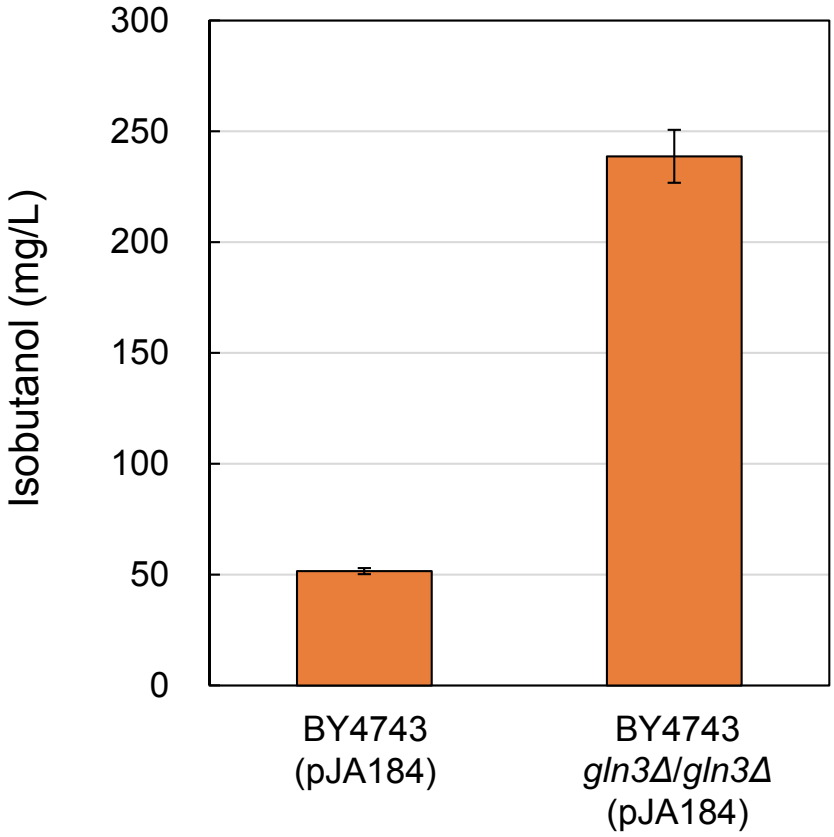

Figure S10. Isobutanol production by isobutanol-tolerant strain with *GLN3* deletion in inhouse-prepared SC-Ura medium (related to Figure 6). Isobutanol production of the homozygous BY4743 *gln3Δ*/*gln3Δ* strain in inhouse-prepared SC-Ura medium (Table S8) compared to wild type BY4743, harboring a 2μ plasmid overexpressing the five enzymes responsible for converting pyruvate to isobutanol in their natural locations (pJA184). Error bars represent the SEM of four independent experiments.

Table S1. Tolerance factors of the wild type BY4741 strain in various concentrations of isobutanol and ethanol (related to Figure 1). OD_{600} values for 0% and 1.4% isobutanol are shown as red point in Figure 1A.

Isobutanol (%)	Tolerance factors of the wild type BY4741
0.6	0.92
1.2	0.72
1.4	0.38
1.5	0.19
1.6	0.11
Ethanol (%)	**Tolerance factors of the wild type BY4741**
8.0	0.31

Table S3. Genes whose deletion leads to sensitivity to isobutanol in the second screen (related to Figure 1B). Gene deletions in hypersensitive strains (TF < 0.5 in 0.6% isobutanol or TF < 0.1 in 1.2% isobutanol) are highlighted in gray.

Systematic name	Common name	Tolerance factor in 0.6% isobutanol	Tolerance factor in 1.2% isobutanol	Tolerance factor in 8% EtOH
YHR183W	*GND1*	0.040	0.057	0.309
YNL241C	*ZWF1*	0.090	0.062	0.344
YCR024C	*SLM5*	0.105	0.044	0.036
YCR028C	*FEN2*	0.130	0.159	0.252
YOR332W	*VMA4*	0.174	0.042	0.158
YBR171W	*SEC66*	0.205	0.104	0.123
YNL064C	*YDJ1*	0.206	0.102	0.095
YER122C	*GLO3*	0.228	0.049	0.028
YLR240W	*VPS34*	0.231	0.034	0.021
YLR304C	*ACO1*	0.316	0.034	0.015
YOR036W	*PEP12*	0.326	0.069	0.119
YDR323C	*PEP7*	0.370	0.040	0.015
YDR495C	*VPS3*	0.377	0.187	0.090
YLR447C	*VMA6*	0.403	0.134	0.036
YBR030W	*RKM3*	0.403	0.771	0.481
YLR244C	*MAP1*	0.424	0.144	0.068
YLL028W	*TPO1*	0.425	0.615	0.389
YJL129C	*TRK1*	0.433	0.143	0.384
YLR138W	*NHA1*	0.437	0.436	0.297
YDR207C	*UME6*	0.440	0.056	0.086
YDR316W	*OMS1*	0.447	0.776	0.431
YCR034W	*ELO2*	0.454	0.215	0.119
YDR315C	*IPK1*	0.476	0.166	0.258
YFL023W	*BUD27*	0.484	0.210	0.172
YDL160C	*DHH1*	0.487	0.147	0.170
YBR018C	*GAL7*	0.513	0.376	0.118
YLR182W	*SWI6*	0.526	0.093	0.093
YEL027W	*VMA3*	0.532	0.151	0.036
YGL173C	*XRN1*	0.536	0.347	0.084
YBR173C	*UMP1*	0.537	0.196	0.149
YHL011C	*PRS3*	0.539	0.106	0.168
YGL168W	*HUR1*	0.560	0.276	0.077
YDR417C	-	0.564	0.465	0.217
YOR035C	*SHE4*	0.573	0.074	0.090
YEL007W	*MIT1*	0.580	0.509	0.440
YLR396C	*VPS33*	0.580	0.113	0.058
YNL236W	*SIN4*	0.586	0.028	0.025
YHR064C	*SSZ1*	0.586	0.263	0.101
YBR024W	*SCO2*	0.586	0.841	0.412
YGL167C	*PMR1*	0.587	0.295	0.079
YBR105C	*VID24*	0.592	0.595	0.291
YDL006W	*PTC1*	0.595	0.173	0.319
YDR320C	*SWA2*	0.596	0.514	0.176
YOR065W	*CYT1*	0.599	0.658	0.140
YKL204W	*EAP1*	0.600	0.324	0.153
YGL026C	*TRP5*	0.601	0.057	0.258
YOR304C-A	*BIL1*	0.604	0.486	0.165
YBR179C	*FZO1*	0.604	0.459	0.164
YKL212W	*SAC1*	0.606	0.211	0.172
YIL076W	*SEC28*	0.612	0.044	0.055
YER111C	*SWI4*	0.618	0.119	0.103

YMR142C	*RPL13B*	0.619	0.132	0.044
YLR372W	*ELO3*	0.619	0.149	0.091
YDL182W	*LYS20*	0.621	0.162	0.368
YGL020C	*GET1*	0.623	0.158	0.319
YOR290C	*SNF2*	0.628	0.023	0.066
YPL060W	*MFM1*	0.633	0.589	0.489
YGL072C	-	0.634	0.241	0.211
YGR257C	*MTM1*	0.644	0.244	0.398
YGR252W	*GCN5*	0.648	0.461	0.151
YCL007C	-	0.650	0.148	0.091
YBR231C	*SWC5*	0.652	0.568	0.302
YLR102C	*APC9*	0.657	0.724	0.735
YDR329C	*PEX3*	0.661	0.688	0.406
YGR105W	*VMA21*	0.661	0.160	0.034
YDR008C	-	0.661	0.045	0.183
YNL171C	-	0.661	0.152	0.085
YBL098W	*BNA4*	0.665	0.771	0.426
YER090W	*TRP2*	0.669	0.038	0.189
YDR293C	*SSD1*	0.670	0.119	0.091
YJR025C	*BNA1*	0.682	0.112	0.059
YGL152C	-	0.684	0.744	0.292
YGR285C	*ZUO1*	0.698	0.280	0.179
YOR322C	*LDB19*	0.704	0.215	0.201
YCL023C	-	0.705	0.586	0.543
YOR008C	*SLG1*	0.708	0.505	0.141
YDR484W	*VPS52*	0.713	0.156	0.118
YKL037W	*AIM26*	0.714	0.347	0.143
YBR221C	*PDB1*	0.720	0.312	0.187
YCR020W-B	*HTL1*	0.721	0.129	0.057
YJL115W	*ASF1*	0.721	0.706	0.198
YJL127C	*SPT10*	0.723	0.802	0.378
YBR068C	*BAP2*	0.727	0.096	0.228
YLR202C	-	0.730	0.041	0.004
YOL023W	*IFM1*	0.731	0.191	0.131
YJL120W	-	0.731	0.182	0.370
YKL118W	-	0.732	0.209	0.070
YHR067W	*HTD2*	0.736	0.159	0.135
YPL002C	*SNF8*	0.737	0.160	0.075
YPR049C	*ATG11*	0.741	0.256	0.113
YDL172C	-	0.744	0.129	0.363
YNL184C	-	0.747	0.425	0.154
YBR003W	*COQ1*	0.748	0.687	0.244
YDR127W	-	0.748	0.022	0.035
YHR026W	*VMA16*	0.753	0.338	0.049
YFL001W	*DEG1*	0.754	0.637	0.337
YKL211C	*TRP3*	0.755	0.071	0.186
YLR047C	*FRE8*	0.757	0.561	0.406
YPL054W	*LEE1*	0.758	0.681	0.545
YLR358C	-	0.762	0.148	0.035
YLR315W	*NKP2*	0.764	0.188	0.270
YJL056C	*ZAP1*	0.774	0.106	0.232
YLR337C	*VRP1*	0.775	0.442	0.137
YMR312W	*ELP6*	0.780	0.335	0.181
YDR101C	*ARX1*	0.782	0.642	0.278
YML121W	*GTR1*	0.784	0.471	0.115
YJL102W	*MEF2*	0.785	0.645	0.224
YER047C	*SAP1*	0.785	0.801	0.678

YJR102C	*VPS25*	0.795	0.263	0.097
YPL045W	*VPS16*	0.796	0.048	0.021
YJL189W	*RPL39*	0.800	0.336	0.203
YGR135W	*PRE9*	0.803	0.550	0.282
YKL119C	*VPH2*	0.809	0.291	0.070
YBR006W	*UGA2*	0.816	0.826	0.519
YJL183W	*MNN11*	0.816	0.122	0.084
YBR036C	*CSG2*	0.819	0.120	0.070
YLR399C	*BDF1*	0.824	0.291	0.091
YNL025C	*SSN8*	0.827	0.371	0.069
YNL055C	*POR1*	0.830	0.154	0.109
YLR233C	*EST1*	0.831	0.159	0.097
YER178W	*PDA1*	0.832	0.545	0.428
YDR078C	*SHU2*	0.850	0.094	0.004
YDL185W	*VMA1*	0.851	0.234	0.029
YGL143C	*MRF1*	0.854	0.055	0.013
YJL180C	*ATP12*	0.854	0.620	0.250
YKL134C	*OCT1*	0.854	0.335	0.292
YLR025W	*SNF7*	0.861	0.248	0.110
YDR354W	*TRP4*	0.863	0.143	0.365
YDR007W	*TRP1*	0.872	0.110	0.272
YDL173W	*PAR32*	0.874	0.136	0.315
YBR212W	*NGR1*	0.877	0.745	0.533
YJL121C	*RPE1*	0.882	0.080	0.287
YLR200W	*YKE2*	0.892	0.694	0.207
YDL116W	*NUP84*	0.895	0.551	0.328
YLR382C	*NAM2*	0.895	0.483	0.190
YJL036W	*SNX4*	0.896	0.351	0.187
YDR027C	*VPS54*	0.897	0.103	0.090
YPR160W	*GPH1*	0.898	0.382	0.088
YOR211C	*MGM1*	0.899	0.499	0.201
YDR418W	*RPL12B*	0.900	0.357	0.192
YDR018C	*-*	0.904	0.647	0.031
YJL176C	*SWI3*	0.906	0.107	0.096
YDL118W	*-*	0.911	0.741	0.366
YPR060C	*ARO7*	0.913	0.050	0.066
YPL040C	*ISM1*	0.920	0.098	0.010
YOR198C	*YOR198C*	0.925	0.761	0.381
YDR193W	*-*	0.929	0.769	0.425
YOR331C	*-*	0.931	0.366	0.062
YJR105W	*ADO1*	0.931	0.071	0.115
YJL095W	*BCK1*	0.939	0.177	0.336
YGL148W	*ARO2*	0.942	0.048	0.061
YDR058C	*TGL2*	0.945	0.274	0.339
YNL315C	*ATP11*	0.956	0.417	0.259
YPR074C	*TKL1*	0.966	0.617	0.623
YKR001C	*VPS1*	0.979	0.297	0.138
YGR163W	*GTR2*	0.982	0.544	0.159
YOR221C	*MCT1*	0.992	0.438	0.262
YOL006C	*TOP1*	0.996	0.117	0.099
YOR070C	*GYP1*	1.011	0.397	0.299
YOR150W	*MRPL23*	1.013	0.736	0.291
YDR173C	*ARG82*	1.019	0.204	0.069
YOL004W	*SIN3*	1.104	0.423	0.130
YDR162C	*NBP2*	1.119	0.080	0.166
YDR184C	*ATC1*	1.247	0.885	0.441

Table S4. Genes whose deletion confers highest tolerance to isobutanol (related to Figure 1C). Gene deletions in hypertolerant strains (TF > 0.4 in 1.5% isobutanol) are highlighted in gray.

Systematic name	Common name	Tolerance factor in 1.5% isobutanol	Tolerance factor in 1.6% isobutanol	Tolerance factor in 9% EtOH
YER040W	*GLN3*	0.809	0.557	0.267
YJR044C	*VPS55*	0.689	0.355	0.464
YDR508C	*GNP1*	0.507	0.374	0.401
YKL146W	*AVT3*	0.481	0.248	0.037
YKR026C	*GCN3*	0.470	0.300	0.003
YDR391C	-	0.402	0.317	0.408
YLL039C	*UBI4*	0.391	0.251	0.128
YGR144W	*THI4*	0.357	0.224	0.463
YIR005W	*IST3*	0.353	0.175	0.000
YKR052C	*MRS4*	0.303	0.167	0.003
YLR278C	-	0.290	0.138	0.002
YLR280C	-	0.286	0.159	0.002
YOR155C	*ISN1*	0.281	0.128	0.257
YDR514C	-	0.280	0.166	0.315
YKL147C	-	0.271	0.125	0.003
YKL051W	*SFK1*	0.253	0.132	0.323
YGR124W	*ASN2*	0.248	0.180	0.406
YDR134C	-	0.242	0.131	0.337
YDL169C	*UGX2*	0.231	0.118	0.305
YIL024C	-	0.231	0.159	0.148
YLR250W	*SSP120*	0.224	0.118	0.002
YGR016W	-	0.222	0.142	0.330
YLR236C	-	0.216	0.104	0.001
YLR279W	-	0.213	0.105	0.002
YIL085C	*KTR7*	0.211	0.095	0.001
YJL201W	*ECM25*	0.207	0.122	0.297
YPL194W	*DDC1*	0.201	0.132	0.171
YLR225C	-	0.188	0.230	0.397
YPL197C	-	0.180	0.127	0.163
YLR445W	*GMC2*	0.170	0.100	0.003
YLR134W	*PDC5*	0.165	0.113	0.271
YDR421W	*ARO80*	0.158	0.178	0.375
YIL088C	*AVT7*	0.154	0.124	0.159
YDL214C	*PRR2*	0.151	0.079	0.192
YKL072W	*STB6*	0.150	0.090	0.194
YML054C	*CYB2*	0.140	0.087	0.219

Table S5. Gene ontology enrichment analysis of the 164 genes whose deletion causes the highest isobutanol sensitivity (related to Figure 1)

GO term	Cluster frequency	Background frequency	P-value
Aromatic amino acid family biosynthetic process	7 (4.3%)	9 (0.1%)	7.78E-08
Single-organism cellular process	98 (59.8%)	2626 (36.7%)	8.06E-07
Aromatic amino acid family metabolic process	9 (5.5%)	24 (0.3%)	1.04E-06
Single-organism process	107 (65.2%)	3031 (42.3%)	1.39E-06
Tryptophan biosynthetic process	5 (3.0%)	5 (0.1%)	4.58E-06
Indole-containing compound biosynthetic process	5 (3.0%)	5 (0.1%)	4.58E-06
Indolalkylamine biosynthetic process	5 (3.0%)	5 (0.1%)	4.58E-06
Indole-containing compound metabolic process	7 (4.3%)	14 (0.2%)	6.73E-06
Tryptophan metabolic process	7 (4.3%)	14 (0.2%)	6.73E-06
Indolalkylamine metabolic process	7 (4.3%)	14 (0.2%)	6.73E-06
Vacuolar transport	19 (11.6%)	171 (2.4%)	7.24E-06
Cellular monovalent inorganic cation homeostasis	9 (5.5%)	39 (0.5%)	0.00013
Cellular chemical homeostasis	16 (9.8%)	148 (2.1%)	0.00017
Cellular cation homeostasis	14 (8.5%)	115 (1.6%)	0.00023
Cellular biogenic amine metabolic process	7 (4.3%)	22 (0.3%)	0.00029
Monovalent inorganic cation homeostasis	9 (5.5%)	43 (0.6%)	0.00031
Cellular homeostasis	17 (10.4%)	177 (2.5%)	0.00039
Cation homeostasis	14 (8.5%)	123 (1.7%)	0.00054
Cellular biogenic amine biosynthetic process	5 (3.0%)	9 (0.1%)	0.00054
Amine biosynthetic process	5 (3.0%)	9 (0.1%)	0.00054
Cellular amine metabolic process	8 (4.9%)	36 (0.5%)	0.00086
Amine metabolic process	8 (4.9%)	36 (0.5%)	0.00086
Cellular ion homeostasis	14 (8.5%)	128 (1.8%)	0.00087
Small molecule metabolic process	36 (22.0%)	684 (9.5%)	0.00098
Chemical homeostasis	16 (9.8%)	170 (2.4%)	0.00112
pH reduction	7 (4.3%)	27 (0.4%)	0.00136
Intracellular pH reduction	7 (4.3%)	27 (0.4%)	0.00136
Vacuolar acidification	7 (4.3%)	27 (0.4%)	0.00136
Biological regulation	63 (38.4%)	1604 (22.4%)	0.00159
Autophagy	15 (9.1%)	155 (2.2%)	0.00172
Inorganic ion homeostasis	13 (7.9%)	118 (1.6%)	0.00198
Ion homeostasis	14 (8.5%)	138 (1.9%)	0.00217
Regulation of cellular pH	7 (4.3%)	29 (0.4%)	0.00229
Regulation of intracellular pH	7 (4.3%)	29 (0.4%)	0.00229
Protein localization to vacuole	13 (7.9%)	120 (1.7%)	0.00239
Carboxylic acid metabolic process	23 (14.0%)	351 (4.9%)	0.00331
Regulation of pH	7 (4.3%)	32 (0.4%)	0.00466
Oxoacid metabolic process	23 (14.0%)	365 (5.1%)	0.00635
Organic acid metabolic process	23 (14.0%)	365 (5.1%)	0.00664
Cellular component organization	68 (41.5%)	1867 (26.1%)	0.00781

Table S8. Compositions of synthetic complete (SC) media other than glucose (related to STAR Methods)

Components	Final concentration in commercial medium (mg/L)	Final concentration in medium made inhouse (mg/L)
Adenine	18	95
p-Aminobenzoic acid	8	9.5
Ammonium sulfate	5000	5000
Alanine	76	95
Arginine	76	95
Asparagine	76	95
Aspartic acid	76	95
Cysteine	76	95
Glutamic acid	76	95
Glutamine	76	95
Glycine	76	95
Histidine	76	95
Inositol	76	36
Isoleucine	76	95
Leucine	380	190
Lysine	76	95
Methionine	76	95
Phenylalanine	76	95
Proline	76	95
Serine	76	95
Threonine	76	95
Tryptophan	76	95
Tyrosine	76	95
Uracil	76	95
Valine	76	95
Yeast nitrogen base without amino acids	1700	1500

Table S9. Yeast strains used in this study (related to STAR Methods)

Strain	Genotype	Source
BY4741	S288C *MAT***a** *his3Δ1 leu2Δ0 met15Δ0 ura3Δ0*	Euroscarf: Y00000
BY4743	S288C *MAT***a**/α *his3Δ1/his3Δ1 leu2Δ0/leu2Δ0 LYS2/lys2Δ0 met15Δ0/MET15 ura3Δ0/ura3Δ0*	Euroscarf: Y20000
CEN.PK2-1C	*MAT***a** *his3Δ1 leu2-3,112 ura3-52 trp1-289 MAL2-8^{c} SUC2*	Euroscarf: 30000A
SEY6210	*MAT*α *leu2-3,112 ura3-52 his3-Δ200 trp1-Δ 901 suc2-Δ9 lys2-801 GAL*	ATCC: 96099
BY4741 *aco1Δ*	BY4741 *aco1Δ::kanMX4*	Euroscarf: Y05212
BY4741 *avt3Δ*	BY4741 *avt3Δ::kanMX4*	Euroscarf: Y04996
BY4741 *dhh1Δ*	BY4741 *dhh1Δ::kanMX4*	Euroscarf: Y03858
BY4741 *elo2Δ*	BY4741 *elo2Δ::kanMX4*	Euroscarf: Y05763
BY4741 *gcn3Δ*	BY4741 *gcn3Δ::kanMX4*	Euroscarf: Y05097
BY4741 *gln3Δ*	BY4741 *gln3Δ::kanMX4*	Euroscarf: Y00173
BY4741 *glo3Δ*	BY4741 *glo3Δ::kanMX4*	Euroscarf: Y06121
BY4741 *gnd1Δ*	BY4741 *gnd1Δ::kanMX4*	Euroscarf: Y02877
BY4741 *ipk1Δ*	BY4741 *ipk1Δ::kanMX4*	Euroscarf: Y07747
BY4741 *map1Δ*	BY4741 *map1Δ::kanMX4*	Euroscarf: Y05153
BY4741 *nha1Δ*	BY4741 *nha1Δ::kanMX4*	Euroscarf: Y04095
BY4741 *pep12Δ*	BY4741 *pep12Δ::kanMX4*	Euroscarf: Y01812
BY4741 *rpe1Δ*	BY4741 *rpe1Δ::kanMX4*	Euroscarf: Y01305
BY4741 *sec28Δ*	BY4741 *sec28Δ::kanMX4*	Euroscarf: Y01469
BY4741 *sec66Δ*	BY4741 *sec66Δ::kanMX4*	Euroscarf: Y03311
BY4741 *sol3Δ*	BY4741 *sol3Δ::kanMX4*	Euroscarf: Y02857
BY4741 *swi6Δ*	BY4741 *swi6Δ::kanMX4*	Euroscarf: Y04131
BY4741 *tal1Δ*	BY4741 *tal1Δ::kanMX4*	Euroscarf: Y05263
BY4741 *tkl1Δ*	BY4741 *tkl1Δ::kanMX4*	Euroscarf: Y05493
BY4741 *trp1Δ*	BY4741 *trp1Δ::kanMX4*	Euroscarf: Y07202
BY4741 *trp2Δ*	BY4741 *trp2Δ::kanMX4*	Euroscarf: Y06395
BY4741 *ume6Δ*	BY4741 *ume6Δ::kanMX4*	Euroscarf: Y03566
BY4741 *vma4Δ*	BY4741 *vma4Δ::kanMX4*	Euroscarf: Y01629
BY4741 *vma6Δ*	BY4741 *vma6Δ::kanMX4*	Euroscarf: Y06051
BY4741 *vps34Δ*	BY4741 *vps34Δ::kanMX4*	Euroscarf: Y05149
BY4741 *vps3Δ*	BY4741 *vps3Δ::kanMX4*	Euroscarf: Y04329
BY4741 *vps55Δ*	BY4741 *vps55Δ::kanMX4*	Euroscarf: Y06842
BY4741 *ydj1Δ*	BY4741 *ydj1Δ::kanMX4*	Euroscarf: Y03012
BY4741 *ydr391cΔ*	BY4741 *ydr391cΔ::kanMX4*	Euroscarf: Y04227
BY4741 *ynl170wΔ*	BY4741 *ynl170wΔ::kanMX4*	Euroscarf: Y02041
BY4741 *zwf1Δ*	BY4741 *zwf1Δ::kanMX4*	Euroscarf: Y01971
BY4742 *gnd1Δ*	BY4742 *gnd1Δ::kanMX4*	Euroscarf: Y12877
BY4742 *zwf1Δ*	BY4742 *zwf1Δ::kanMX4*	Euroscarf: Y11971
BY4743 *gln3Δ/gln3Δ*	BY4743 *gln3Δ::kanMX4/gln3Δ::kanMX4*	Euroscarf: Y30173
CEN.PK2-1C *TRP1*	CEN.PK2-1C *TRP1*	This study
CEN.PK2-1C *TRP1 gln3Δ*	CEN.PK2-1C *TRP1 gln3Δ::kanMX4*	This study
CEN.PK2-1C *TRP1 gnd1Δ*	CEN.PK2-1C *TRP1 gnd1Δ::kanMX4*	This study
CEN.PK2-1C *TRP1 zwf1Δ*	CEN.PK2-1C *TRP1 zwf1Δ::kanMX4*	This study

SEY6210 *TRP1*	SEY6210 *TRP1*	This study
BY4741 (pRS426)	BY4741 pRS426	This study
BY4741 (*GND1*)	BY4741 pXP684-GND1	This study
BY4741 (*GND2*)	BY4741 pXP684-GND2	This study
BY4741 (*RPE1*)	BY4741 pXP684-RPE1	This study
BY4741 (*SOL3*)	BY4741 pXP684-SOL3	This study
BY4741 (*TAL1*)	BY4741 pXP684-TAL1	This study
BY4741 (*TKL1*)	BY4741 pXP684-TKL1	This study
BY4741 (*TKL2*)	BY4741 pXP684-TKL2	This study
BY4741 (*ZWF1*)	BY4741 pXP684-ZWF1	This study
BY4741 (pJA184)	BY4741 pJA184 (*ILV2*, *ILV3*, *ILV5*, *LlKivD*, *ADH7*)	This study
BY4741 *gln3Δ* (pRS426)	BY4741 *gln3Δ::lox66-natMX6-lox71* pRS426	This study
BY4741 *gln3Δ* (pJA184)	BY4741 *gln3Δ::lox66-natMX6-lox71* pJA184 (*ILV2*, *ILV3*, *ILV5*, *LlKivD*, *ADH7*)	This study
BY4741 *ald6Δ* (pRS426)	BY4741 *ald6Δ::loxP-kanMX4-loxP* pRS426	This study
BY4741 *ald6Δ* (pJA184)	BY4741 *ald6Δ::loxP-kanMX4-loxP* pJA184 (*ILV2*, *ILV3*, *ILV5*, *LlKivD*, *ADH7*)	This study
BY4741 *ald6Δ gln3Δ* (pRS426)	BY4741 *gln3Δ::lox66-natMX6-lox71 ald6Δ::loxP-kanMX4-loxP* pRS426	This study
BY4741 *ald6Δ gln3Δ* (pJA184)	BY4741 *gln3Δ::lox66-natMX6-lox71 ald6Δ::loxP-kanMX4-loxP* pJA184 (*ILV2*, *ILV3*, *ILV5*, *LlKivD*, *ADH7*)	This study
BY4743 (pRS426)	BY4743 pRS426	This study
BY4743 *gln3Δ/gln3Δ* (pRS426)	BY4743 *gln3Δ::kanMX4/gln3Δ::kanMX4* pRS426	This study
BY4743 (pJA184)	BY4743 pJA184 (*ILV2*, *ILV3*, *ILV5*, *LlKivD*, *ADH7*)	This study
BY4743 *gln3Δ/gln3Δ* (pJA184)	BY4743 *gln3Δ::kanMX4/gln3Δ::kanMX4* pJA184 (*ILV2*, *ILV3*, *ILV5*, *LlKivD*, *ADH7*)	This study

Table S10. Plasmids used in this study (related to STAR Methods)

Plasmid	Description	Source
pXP684-GND1	Overexpression of *GND1* by 2µ *URA3* plasmid containing the endogenous promoter, ORF, and terminator sequence	Huang et al., 2013
pXP684-GND2	Overexpression of *GND2* by 2µ *URA3* plasmid containing the endogenous promoter, ORF, and terminator sequence	Huang et al., 2013
pXP684-RPE1	Overexpression of *RPE1* by 2µ *URA3* plasmid containing the endogenous promoter, ORF, and terminator sequence	Huang et al., 2013
pXP684-SOL3	Overexpression of *SOL3* by 2µ *URA3* plasmid containing the endogenous promoter, ORF, and terminator sequence	Huang et al., 2013
pXP684-TAL1	Overexpression of *TAL1* by 2µ *URA3* plasmid containing the endogenous promoter, ORF, and terminator sequence	Huang et al., 2013
pXP684-TKL1	Overexpression of *TKL1* by 2µ *URA3* plasmid containing the endogenous promoter, ORF, and terminator sequence	Huang et al., 2013
pXP684-TKL2	Overexpression of *TKL2* by 2µ *URA3* plasmid containing the endogenous promoter, ORF, and terminator sequence	Huang et al., 2013
pXP684-ZWF1	Overexpression of *ZWF1* by 2µ *URA3* plasmid containing the endogenous promoter, ORF, and terminator sequence	Huang et al., 2013
pRS426	Empty plasmid with 2µ and *URA3*	ATCC: 96099
pJA184	Isobutanol production by 2µ *URA3* plasmid containing P_{TDH3}-*ILV2-HA*-T_{ADH1}, P_{PGK1}-*ILV3-His*-T_{CYC1}, P_{TEF1}-*ADH7-Myc*-T_{ACT1}, [P_{TEF1}-*ILV5*-*Myc*-T_{ACT1}, P_{TDH3}-*LlKivD*-*HA*-T_{ADH1}]	Avalos et al., 2013
pYZ84	Plasmid containing the *lox66-natMX6-lox71* deletion cassette	Hammer and Avalos, 2017
pUG6	Plasmid containing the *loxP-kanMX4-loxP* deletion cassette	Gueldener et al., 2002

* Brackets indicate reverse compliments.

Table S11. Primers used in this study (related to STAR Methods)

Primer	Sequence (5'–3')	Target region or description
TRP1-Pro-F	ACACTGAGTAATGGTAGTTATAAGAAAGAG	P_{TRP1}-*TRP1*-T_{TRP1}
TRP1-Term-R	TGGTGTTTATGCAAAGAAACCACTGTGTTT	
GLN3-F	TCTTGCAAGACAGAGAAAGATGTTC	5' Flanking sequence of *GLN3*-*KanMX4*-3' flanking sequence of *GLN3*
GLN3-D	AAACAAATAATACCAATGCTCAGGA	
GND1-A	TAAATCACCTGCTACCTCTCTGTTC	5' Flanking sequence of *GND1*-*KanMX4*-3' flanking sequence of *GND1*
GND1-D	TTTTCTGACTTCATGATTTTGTGTC	
ZWF1-A	ATTATTAATGTGGGATTTTTGGCTC	5' Flanking sequence of *ZWF1*-*KanMX4*-3' flanking sequence of *ZWF1*
ZWF1-D	TCAATGATAAGTACAAGTCCAATCG	
ALD6-KO-F	TCTTGTTTTATAGAAGAAAAAACATCAAGAAACATCTTTAACATACACAAACACATACTATCAGAATACATACGCTGCAGGTCGACAACC	5' Flanking sequence of *ALD6*-*KanMX4*-3' flanking sequence of *ALD6*
ALD6-KO-R	GACGTAAGACCAAGTAAGTTTATATGAAAGTATTTTGTGTATATGACGGAAAGAAATGCAGGTTGGTACACTAGTGGATCTGATATCACC	
GLN3-KO-F	ATAACAGAGTGTGTAAGAAAGAGAGACGAGAGAGAGCACAGGGCCCCCTTTTCCCCCACCAACAAACAATACGCTGCAGGTCGACAACC	5' Flanking sequence of *GLN3*-*NatMX6*-3' flanking sequence of *GLN3*
GLN3-KO-R	GAAAATCTATCAATGCAACCGTTCAGTAATTATTAACATAATAAGAATAATGATAATGATAATACGCGGCTAGTGGATFTGATATCACC	
GLN3-F2	TTTGCTCTATTACCCGGCGGACAGG	Forward primer annealing upstream of the introduced DNA fragment for *GLN3* deletion
GND1-A2	CCCTTCTACATAACTCCATGCATGC	Forward primer annealing upstream of the introduced DNA fragment for *GND1* deletion
ZWF1-A2	TGCTAAAAGCCCGGTTTCGGCTCGG	Forward primer annealing upstream of the introduced DNA fragment for *ZWF1* deletion
ALD6-F	GGGATTCAAGACAAGCAACCTTGTTAGTCA	Forward primer annealing upstream of the introduced DNA fragment for *ALD6* deletion
Jla_oli239	ATTCGTCGTCGGGGAACACC	Reverse primer annealing within *NatMX6*
JW38	GCACGTCAAGACTGTCAAGG	Reverse primer annealing within *KanMX4*

Table S12. Analytical methods to quantify amino acids by LC-MS/MS (related to STAR Methods)

Amino acid	Compound abbreviation	MRM transition	Q1 Pre Bias (V)	Q3 Pre Bias (V)	Collision energy (V)	Retention time (min)
L-Glutamic acid	E	148.1>130.1	-29	-2	-1	2.81
L-Glutmaine	Q	147.1>56.2	-3	-2	-32	2.48
L-Glutamic acid-$^{13}C_5$,^{15}N		154.1>89.0	-29	-17	-2	2.81
L-Glutamine-$^{13}C_5$,$^{15}N_2$		154.1>60.0	-3	-2	-32	2.47